The variability of root cohesion as an influence on shallow landslide ...
Schmidt, K M;Roering, J J;Stock, J D;Dietrich, W E;et al
Canadian Geotechnical Journal; Oct 2001; 38, 5; ProQuest Central
pg. 995

995

The variability of root cohesion as an influence on shallow landslide susceptibility in the Oregon Coast Range

K.M. Schmidt, J.J. Roering, J.D. Stock, W.E. Dietrich, D.R. Montgomery, and T. Schaub

Abstract: Decades of quantitative measurement indicate that roots can mechanically reinforce shallow soils in forested landscapes. Forests, however, have variations in vegetation species and age which can dominate the local stability of landslide-initiation sites. To assess the influence of this variability on root cohesion we examined scarps of landslides triggered during large storms in February and November of 1996 in the Oregon Coast Range and hand-dug soil pits on stable ground. At 41 sites we estimated the cohesive reinforcement to soil due to roots by determining the tensile strength, species, depth, orientation, relative health, and the density of roots ≥ 1 mm in diameter within a measured soil area. We found that median lateral root cohesion ranges from 6.8–23.2 kPa in industrial forests with significant understory and deciduous vegetation to 25.6–94.3 kPa in natural forests dominated by coniferous vegetation. Lateral root cohesion in clearcuts is uniformly ≤ 10 kPa. Some 100-year-old industrial forests have species compositions, lateral root cohesion, and root diameters that more closely resemble 10-year-old clearcuts than natural forests. As such, the influence of root cohesion variability on landslide susceptibility cannot be determined solely from broad age classifications or extrapolated from the presence of one species of vegetation. Furthermore, the anthropogenic disturbance legacy modifies root cohesion for at least a century and should be considered when comparing contemporary landslide rates from industrial forests with geologic background rates.

Key words: root strength, cohesion, landslide, debris flow, land use, anthropogenic disturbance.

Résumé : Des décades de mesures quantitatives indiquent que les racines peuvent renforcer mécaniquement les sols de surface dans des paysages boisés. Cependant, les forêts ont des variations d'espèces et d'âge qui peuvent dominer la stabilité locale des sites d'initiation de glissements. Pour évaluer l'influence de cette variabilité sur la cohésion due aux racines, on a examiné les escarpements des glissements déclenchés durant de gros orages en février et novembre 1996 dans le Oregon Coast range et dans des fosses creusées à la main dans le terrain stable. Sur 41 sites, on a estimé le renforcement du sol dû à la cohésion fournie par les racines en déterminant la résistance en traction, les espèces, la profondeur, l'orientation, la santé relative, et la densité des racines ≥ 1 mm de diamètre à l'intérieur d'une surface mesurée de sol. On a trouvé que la cohésion médiane latérale variait de 6,8 – 23,2 kPa dans les forêts industrielles en revégétation caduque significative, à 25,6 – 94,3 kPa dans les forêts naturelles dominées par une végétation de conifères. La cohésion latérale des racines dans des coupes nettes est uniformément ≤ 10 kPa. Des forêts industrielles vieilles de 100 ans ont des compositions d'espèces, une cohésion latérale de racines, et des diamètres de racines qui ressemblent plus à des coupes à blanc de 10 années qu'à des forêts naturelles. Comme telle, l'influence de la variabilité de la cohésion due aux racines sur la susceptibilité au glissement ne peut pas être déterminée seulement sur la base des classifications générales d'âge ou extrapolée en partant de la présence d'une espèce de végétation. De plus, l'héritage des remaniements anthropogéniques modifie la cohésion due aux racines pour au moins un siècle et devrait être pris en considération lorsque l'on compare la fréquence des glissements contemporains dans les forêts industrielles aux fréquences des glissements d'âge géologique.

Mots clés : résistance des racines, cohésion, glissement, coulée de débris, utilisation des terres, remaniement anthropogénique.

[Traduit par la Rédaction]

K.M. Schmidt.[1] U.S. Geological Survey, 345 Middlefield Road, MS 975, Menlo Park, CA 94025, U.S.A.
J.J. Roering. Department of Geological Sciences, University of Oregon, Eugene, OR 97403–1272, U.S.A.
J.D. Stock, and W.E. Dietrich. Earth and Planetary Science, University of California, Berkeley, CA 94720, U.S.A.
D.R. Montgomery and T. Schaub. Department of Earth and Space Sciences, University of Washington, Box 351310, Seattle, WA 98195, U.S.A.
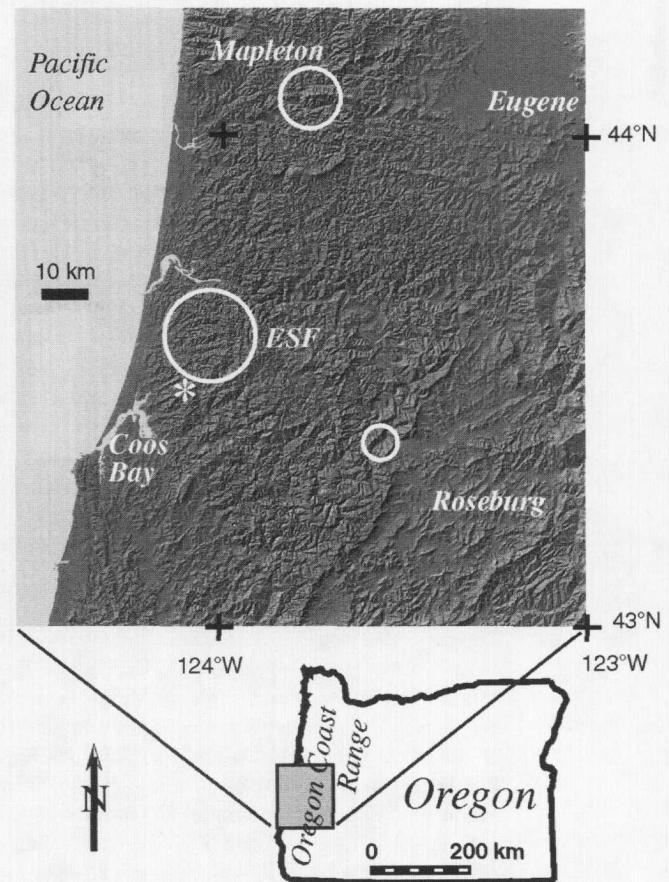
[1]Corresponding author. (e-mail: kschmidt@usgs.gov).

Introduction

Observations of regional patterns in landsliding triggered by large-magnitude storms typically reveal substantial variability in both the locations of landslides within a landscape and the species composition and density of neighboring vegetation. Site-specific field studies commonly exhibit broken roots within landslide scarps, indicating that the presence of the roots modified the shear resistance of the hillslope. The research presented here was motivated by such field observations following storms during 1996 in the Oregon Coast Range (Taylor 1997) which caused thousands of landslides (Robison et al. 1999), loss of human life, and subsequent controversy over land management practices. A storm in February 1996 triggered numerous landslides and associated debris flows in the central and northern portions of the coast range, including the Mapleton area in Fig. 1. According to the Laurel Mountain, Oregon, rain gauge (part of the National Oceanic and Atmospheric Administration – National Weather Service (NOAA–NWS) cooperative observer network) north of the Mapleton study area, the 6–9 February 1996 storm produced 27.88 in. (708 mm) of rain, with a maximum daily total of 8.20 in. (208 mm) (Taylor 1997). During November 1996, another severe storm hit the southern Oregon Coast Range, triggering widespread landsliding from Coos Bay east towards Roseburg (Fig. 1) and causing six fatalities. Our own unpublished rain-gauge measurements on Mettman Ridge in the Coos Bay area (asterisk in Fig. 1) document that the storm of 16–18 November 1996 produced 225 mm of rain, with a maximum daily total of over 150 mm. Field observations in response to these storms revealed numerous broken roots within the slide scarps and substantial variability of the surrounding vegetation in a variety of land-use types, including unharvested, old-growth stands of natural forests; mature second-growth stands in commercially harvested industrial forests; recent clearcuts; and recent clearcuts treated with herbicide intended to eradicate understory vegetation and deciduous trees.

Where storms produce landslides in forested terrain, the pattern of failures is rarely correlated solely with any single measure of forest cover or topography. For instance, digital terrain-based models that estimate landslide susceptibility consistently predict larger, more numerous potential landslides than observed (Carrara et al. 1991; Ellen et al. 1993; Montgomery and Dietrich 1994; Montgomery et al. 1998). Researchers often attribute the seemingly stochastic occurrence of landslides to the spatial variations of topography, soil depth, cohesion from the soil and roots, hydraulic conductivity, groundwater response, and angle of internal friction (Dietrich et al. 1995; Wu and Sidle 1995; Montgomery et al. 1997). In addition, forest clearing can increase the frequency of landsliding (e.g., Sidle et al. 1985), and in southwestern Oregon contemporary landslide rates and sediment yields in areas of recent clear-cut timber harvesting are several times preindustrial rates (Brown and Krygier 1971; Ketcheson and Froelich 1978; Swanson et al. 1991; Amaranthus et al. 1985; Montgomery et al. 2000). Unfortunately, these variables are exceedingly difficult to measure and few studies have attempted to measure their spatial variation at the scale that influences slope stability. From more than two decades of research, though, it is clear that the binding action of roots can profoundly increase the stability

Fig. 1. Shaded relief map showing study areas (open circles and asterisk) in the central Oregon Coast Range where thousands of landslides occurred during winter storms of 1996. The study areas are the Mapleton District, the Elliot State Forest (ESF), Mettman Ridge (represented by the asterisk) northeast of Coos Bay, and the region northwest of Roseburg that includes the landslide and associated debris flow that caused four fatalities on 18 November 1996.

of granular, friction-dominated soils on steep slopes. Hence, root-cohesion variability across the landscape provides a means to significantly alter spatial patterns of landslide susceptibility.

Roots produce an apparent cohesion via root fiber reinforcement (here referred to as root cohesion) that promotes slope stability in shallow soils. The stabilizing reinforcement of roots in soil is supported by landslide inventories that note an increase in landslide frequency following vegetation removal (Bishop and Stevens 1964; Gray and Megahan 1981; Kuruppuarachchi and Wyrwoll 1992); accelerated displacement of existing landslides following vegetation conversion (DeGraff 1979; Swanston 1988); laboratory experiments on rooted, artificially reinforced, and fallow soil (Endo and Tsuruta 1969; Waldron 1977; Waldron and Dakessian 1981, 1982; Waldron et al. 1983); slope stability analyses of field data (Swanston 1970; Burroughs and Thomas 1977; Ziemer and Swanston 1977; Wu et al. 1979; Riestenberg and Sovonick-Dunford 1983; Reneau and Dietrich 1987; Terwilliger and Waldron 1991; Riestenberg 1994); and numerical modeling analyses (Wu et al. 1988a, 1988b; Sidle 1992; Krogstad 1995).

© 2001 NRC Canada

The effect of spatially variable root reinforcement on the pattern of landsliding is difficult to measure with any simple proxy. Although root cohesion likely varies with vegetation type or age, considerable spatial and temporal variation exists in the mosaic of stand density and vegetation composition in forests. The vegetation at a landslide-initiation site may vary with local growing conditions and the legacy of tree senescence, fire, climate change, disease, grazing, or logging (Franklin and Dyrness 1969). This mosaic is dynamic in time and space, with a continual turnover of individuals and species in response to external forcing factors. Since the network of roots depends on the aboveground vegetation mosaic, the apparent cohesion provided by roots to the soil is strongly tied to the legacy of the land.

Root cohesion values are typically back-calculated because field measurements are time consuming and regional coverage is difficult to obtain. However, back-analysis of root cohesion in landslides presumes knowledge of material properties and hydrologic conditions which is rarely verifiable. Values from individual sites are difficult to extrapolate because the growth habits of trees are highly variable, even within a single species growing in different environments (Stout 1956; Coppin and Richards 1990; Stone and Kalisz 1991), and root-thread diameter, density, geometry, and relative health are highly diverse (Wu 1995). It is difficult to predict the variation of root cohesion at different scales because root morphology and distribution reflect both biological mechanisms and their disruption by environmental factors (Dean and Ford 1983). Furthermore, documented root distributions and morphologies are highly variable (Rigg and Harrar 1931; Ross 1932; Bannan 1940; Stout 1956; McMinn 1963; Kochenderfer 1973; Smith 1964; Eis 1974, 1987; Böhm 1979; Watson and O'Loughlin 1990; Phillips and Watson 1994). Although ranges of root cohesion values have been determined for different species of vegetation (e.g., Endo and Tsuruta 1969; Burroughs and Thomas 1977; Wu et al. 1979; Ziemer 1981; Riestenberg and Sovonick-Dunford 1983; Riestenberg 1994), single values representing vegetation communities are typically adopted for regional slope stability calculations. The adoption of constant root cohesion, however, may be inappropriate where root distributions vary spatially. For an unharvested forest of the Oregon Coast Range, Burroughs and Thomas (1977) hypothesized that forest landslides occur within gaps of low root reinforcement or in areas where the root-thread strength declined substantially due to decay. After timber harvest, the interconnected network of a living root system decreases in both density and strength, leaving unreinforced areas around the lateral edges of individual tree-root systems. If substantiated, this observation would improve the understanding of why certain portions of the landscape generate landslides in a storm while others remain stable.

With the aim of explaining some of the spatial pattern of landsliding, we quantified local root cohesion over the Oregon Coast Range in landslides triggered during large storms of 1996 and within pits on stable ground to address the following questions:

(1) Is root reinforcement within a forest so variable that simple age classifications fail to adequately represent root cohesion?

(2) Is there a relationship between root cohesion and average vegetation condition?

(3) How long is the period of root-cohesion recovery following stand disturbance or replacement?

(4) On a regular rotation interval of clear-cutting, will industrial forests attain cohesive reinforcement from roots similar to those of old-growth forests?

Theory

Following the work of Endo and Tsuruta (1969), O'Loughlin (1974), and Waldron (1977), we assume the primary influence of root reinforcement can be expressed as a cohesion term in the Coulomb failure criteria (e.g., Terzaghi 1950) where the soil–root composite shear strength, S_{sr}, is expressed by

$$[1] \qquad S_{sr} = c_s' + c_r + (\sigma - u)\tan \phi'$$

where c_s' is the effective cohesion of the soil, c_r is the apparent cohesion provided by roots, σ is the normal stress due to the weight of the soil and water of the sliding mass, u is the soil pore-water pressure, and ϕ' is the effective internal friction angle of the soil that is unaltered by the presence of roots (e.g., O'Loughlin and Ziemer 1982; Wu 1995). Forest soils typically consists of root fibers of high tensile strength and adhesion in a granular matrix of soil with much lower tensile strength. Roots increase the strength of the soil–root mass by enhancing the confining stress and resistance to sliding (e.g., Waldron 1977). If root threads rupture in tension and (or) shear or if the strength of the root–soil bond is exceeded and roots pull out of the soil matrix, this strength increase vanishes.

We quantify the interaction between root threads and the soil matrix such that root cohesion is limited by the thread strength of the roots themselves, not the bond between the roots and soil. We adopt this procedure and the following equations for determining the increase in shear strength from Wu (1976), Waldron (1977), and Wu et al. (1979). The tensile force at failure of a root thread is expressed as TF_r, and the tensile strength of an individual root thread, T_{ri}, is defined so that
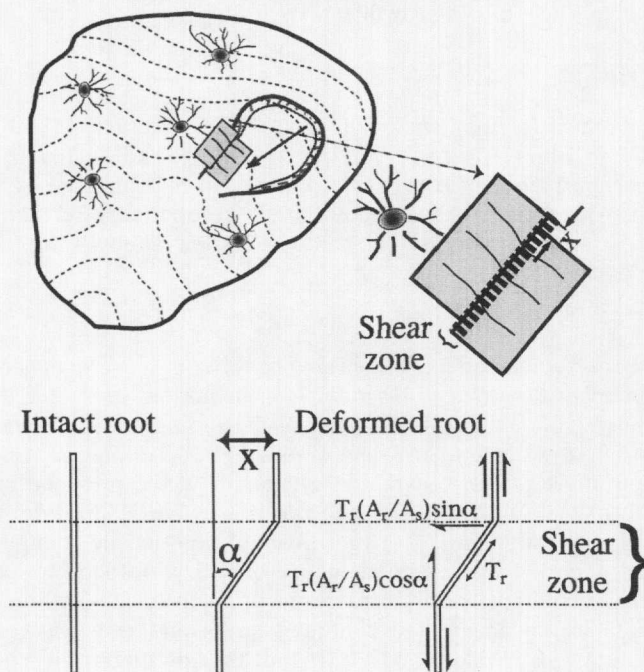
$$[2] \qquad T_{ri} = g \frac{TF_r}{A_{ri}}$$

where g is the gravitational acceleration, and A_{ri} is the cross-sectional area of the root. Assuming the roots cross a shear zone perpendicularly and the ultimate thread strength is mobilized, the total tensile root-thread strength of a given species per unit area of soil, t_r, is expressed as

$$[3] \qquad t_r = \sum_{i=1}^{n} T_{ri}\left(\frac{A_{ri}}{A_s}\right)$$

where A_{ri}/A_s is the root area ratio or proportion of root cross-sectional area to soil cross-sectional area (A_s), and n is the number of roots in area A_s. The ratio of the total cross-sectional area of all roots to soil cross-sectional area is expressed by A_r/A_s. In Fig. 2, the horseshoe-shaped landslide deforms flexible, elastic roots extending perpendicularly across a shear zone, displaced laterally by an amount X, and distorted by angle of shear α. The mobilization of tensile re-

Fig. 2. Plan-form view of idealized topography with cross sections of tree trunks and roots emanating toward a shear zone on the margin of a landslide. Root reinforcement model shows roots oriented perpendicular to the shear zone. For a definition of the variables see the discussion with eqs. [1]–[5]. Modified from Wu (1976) and Gray and Ohashi (1983).

sistance in the fibers in the soil can be translated into a tangential component ($t_r \cos\alpha \tan\phi'$) and a normal component ($t_r \sin\alpha$). Expressed as a thread strength per unit area of soil, the root cohesion is

$$[4] \qquad c_r = t_r(\cos\alpha \tan\phi' + \sin\alpha)$$

Sensitivity analyses indicate that values of $\cos\alpha \tan\phi' + \sin\alpha$ in eq. [4] can be approximated as 1.2 for $25° < \phi' < 40°$ and $40° < \alpha < 70°$ (e.g., Wu 1976; Wu et al. 1979). Values of ϕ' for the coarse-grained colluvium at our field sites in the Oregon Coast Range (described later in the paper) generally vary between 35° and 44° (Yee and Harr 1977; Schroeder and Alto 1983; Burroughs 1985; Wu et al. 1988a). Results of Waldron (1977) and Wu et al. (1979) confirm that α varies at most between 45° and 70°. In addition, experimental direct shear tests on dry, fiber-reinforced sand by Gray and Ohashi (1983) indicate that the greatest reinforcement occurs when a fiber is oriented at 60° with respect to the deformation zone. It is unclear how saturated conditions may alter α and relative fiber reinforcement. Equation [4] is modified to determine the total root cohesion arising from root reinforcement of a given species, such that

$$[5] \qquad c_r = 1.2 \sum_{i=1}^{n} T_{ri}\left(\frac{A_{ri}}{A_s}\right)$$

Greater values of c_r arise from high-strength root threads, larger diameter roots, and (or) increased root densities.

In composite materials, such as a soil reinforced by root fibers, loss of root cohesion can also occur by debonding failure or root slippage, such that the pull-out resistance of the bond between the root and soil is less than the root-thread strength. From laboratory experiments Waldron and Dakessian (1981) concluded that root slippage rather than breakage was a limiting condition of root reinforcement in fine-textured soils. The force, F_p, required to break the soil–root bond, μ, along a length of root, L, for dry conditions can be approximated as

$$[6] \qquad F_p = \pi d\mu L$$

where d is the root diameter, and πd is the perimeter of the root (e.g., Ennos 1990). Field experiments by Anderson et al. (1989) and Riestenberg (1994) support the relation expressed by eq. [6]. For a given diameter, the length of root stressed increases with an increase in the force required for debonding failure. It is difficult, however, to quantify soil–root pull-out resistance over large areas because of the branching, lateral network of roots, presence of root hairs, and interlocking nature of roots from separate plants. The widespread presence of broken roots within landslide scarps in our field area, though, indicates that the pull-out resistance exceeded the root-thread strength, otherwise the roots would have pulled completely out of the soil matrix, revealing unbroken root networks. We suspect that root breakage begins with partial debonding between the soil–root interface followed by root-thread failure. In highly branched root systems, the density of roots per unit area of soil may enable tension to be transferred rapidly to the soil via shear before root pull out occurs (e.g., Ennos 1990).

On the basis of our field observations, laboratory research, and previously published research, we make the following assumptions in the ensuing analyses:

(1) The tensile strength of individual root fibers is fully mobilized (not just bond failure between the soil and root). Our calculation of root cohesion includes only those roots in landslide scarps which broke as a result of landsliding, evidence that their strength was fully mobilized. We may, however, overestimate root cohesion for hand-dug pits because we include all root threads intersecting the walls of the pit, not solely the subset of roots that broke in response to landsliding. This overestimation is likely offset by the fact that we omit the pull-out resistance of the unbroken roots in landslide scarps which also increases relative root cohesion.

(2) The effective internal friction angle, ϕ', is unaffected by root reinforcement. Although laboratory analyses by Endo and Tsuruta (1969) substantiate assumption 2, it is unclear how scale effects modify the contribution to the soil mass frictional strength in the field.

(3) All broken roots failed simultaneously. During landsliding, it is unlikely that all roots are simultaneously loaded to their ultimate tensile strength, hence we may overestimate root cohesion in landslides characterized by slow deformations where roots progressively fail over time. Field measurements of root extraction by Riestenberg (1994) indicate that branches of a root break sequentially as roots are displaced within the soil. Roots aligned parallel to the direction of maximum tensile force receive the largest load and fail first. When a large amount of multibranched root material is present, as with many species of vegetation in the study area, the applied load causes the soil–root mass to behave as a unit (Coutts 1983). Furthermore, all the landslides

investigated in this study mobilized into debris flows and thus we infer that most initiated rapidly in response to high-intensity rainfall with quasi-synchronous failure of the root threads.

(4) Roots are flexible and are initially oriented perpendicular to the shear zone (Fig. 2). Laboratory tests reveal that reinforcing fibers oriented perpendicular to a shear zone provide reinforcement comparable to that of randomly oriented fibers (Gray and Ohashi 1983).

(5) Root cohesion increases are directly proportional to A_r/A_s. Field measurements of root extraction force (Anderson et al. 1989; Riestenberg 1994) and laboratory analyses on the effects of roots on shearing resistance (Kassiff and Kopelovitz 1968; Waldron and Dakessian 1982; Gray and Ohashi 1983) substantiate this assumption, as root reinforcement expresses a positive relationship with root cross-sectional area. The results of Gray and Ohashi (1983) indicate that shear strength increases are directly proportional to A_r/A_s, whereas Jewell and Wroth (1987) and Shewbridge and Sitar (1989) argue that the strength increase in reinforced soil is slightly nonlinear. That is, we may overestimate root cohesion at sites with high root densities (values of $A_r/A_s > 0.005$).

(6) The potential effect of pore-water pressure on c_r is neglected. We also neglect any variation in c_r arising from changes in surface tension in the unsaturated zone.

(7) Root cohesion neglects the bending moments of the individual root threads. Experiments by Shewbridge and Sitar (1990) indicate that methods based on the development of tension within the reinforcing fibers (neglecting bending moments) are sufficient to represent root reinforcement.

In summary, our estimates of c_r may overestimate values for pits where we quantify reinforcement based on all roots intersecting the pit walls and at sites that experienced slow, progressive strain where individual branches of a root network break sequentially. Our field observations taken prior to root decay and landslide scar degradation, though, confirm that the majority of roots intersecting landslide scarps broke in response to landslide deformation. The resulting estimate of c_r is used in slope stability analyses and provides a systematic measure of relative root reinforcement in different land-use types and vegetation conditions. Although more complex root reinforcement models exist, they often require time-consuming excavations to document the branching character of the root network (e.g., Wu et al. 1988b). As our goal was to document the variability of c_r over large areas at a great number of sites, we adopted a simple model employing data obtained by field measurements.

Slope stability and hydrologic modeling

As hydrologic response to rain and slope stability vary across the landscape with topographic curvature, hillslope gradient, and soil properties, we incorporated site-specific representations of the topography into an idealized hydrologic routing model. Field measurements of the local topography surrounding landslide scarps were used to evaluate differences in the measured root cohesion and back-calculated hydrologic conditions at failure. Here the terms landslide scarp or main scarp are used in accordance with Cruden and Varnes (1996) such that they represent a steep surface on undisturbed ground at the upper edge of a land-slide caused by movement of displaced material away from the undisturbed ground.

Shallow-soil slope stability is typically approximated as the one-dimensional case where root cohesion is limited to the unique case of basal anchoring. Numerous researchers, however, recognize that an infinite slope approximation ignores the contribution of roots along the perimeter of a landslide mass (Riestenberg and Sovonick-Dunford 1983; Wu 1984a; Burroughs 1985; Reneau and Dietrich 1987; Terwilliger and Waldron 1991). Our own field observations document that the majority of roots in the Oregon Coast Range grow slope parallel, with few anchoring into the bedrock surface. Therefore we adopt an expanded one-dimensional stability analysis that includes cohesion acting over both a basal surface and the lateral perimeter of a landslide source volume. The influence of buttressing and arching on the soil arising from root mats is neglected because we cannot reproduce the prelandslide configuration of trees with variable diameters and associated roots within the land-slide.

The shear stress, τ, acting over the basal area of the land-slide, A_b, is represented by

[7] $\qquad \tau = A_b \rho_s g z \, \sin\theta \, \cos\theta$

where ρ_s is the saturated sediment bulk density, z is the vertical colluvium thickness, and θ is the ground surface slope. Expanding on eq. [1], the resisting force is approximated as

[8] $\qquad S_{sr} = c_l A_l + c_b A_b + A_b(\rho_s - \rho_w M)gz \, \cos^2\theta \, \tan\phi'$

where c_l is the sum of the effective soil cohesion (c_{sl}') and the root cohesion (c_{rl}) along the perimeter with lateral area A_l, c_b is the basal cohesion comprised of the sum of effective soil cohesion (c_{sb}') and the root cohesion (c_{rb}), ρ_w is the bulk density of water, and M is the ratio of the height of the piezometric surface above the base of the colluvium (h) to the total vertical colluvium thickness (z). This approach neglects lateral earth pressure and the frictional components of resistance along A_l. At a factor of safety of unity, $\tau = S_{sr}$ and landsliding occurs. Solving for the critical proportion of saturated regolith necessary to trigger landsliding, M_c, yields
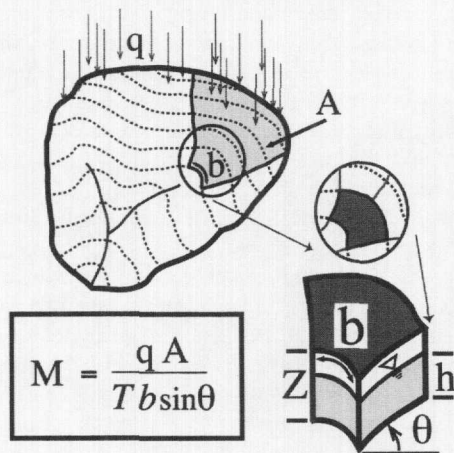
[9] $\quad M_c =$

$$\frac{c_l A_l + c_b A_b + A_b \rho_s g z_s \cos^2\theta \tan\phi' - A_b \rho_s g z \sin\theta \cos\theta}{A_b \rho_w g z \cos^2\theta \tan\phi'}$$

Gathering similar terms results in

[10] $\qquad M_c = \dfrac{c_l A_l + c_b A_b}{A_b \rho_w g z \cos^2\theta \tan\phi'} + \dfrac{\rho_s}{\rho_w}\left(1 - \dfrac{\tan\theta}{\tan\phi'}\right)$

The simple hydrologic model used here to determine the relative degree of saturation estimates steady-state, shallow subsurface flow driven by local topographic controls (O'Loughlin 1986) and follows the subsequent development by Dietrich et al. (1992). This model includes variables (upslope drainage area, contour width through which water in the upslope drainage area flows, and upslope gradient) that can be extracted from digital elevation models or, as obtained here, measured in the field (Fig. 3). In Fig. 3 the idealized topography receives a steady-state rainfall q (rain-

Fig. 3. Conceptual hydrologic model used to infer the relative degree of saturation. Lateral root cohesion measurements were obtained in landslides or pits defining b. See discussion associated with eqs. [11]–[13] for description of variables.

$$M = \frac{qA}{Tb\sin\theta}$$

fall minus evapotranspiration with no leakage into the bedrock) that contributes to an upslope drainage area A and flows through contour length b. The depth-integrated, saturated soil transmissivity (assumed to be constant) is T. Discharge of water, Q, through the regolith is defined as

[11] $\quad Q = q\dfrac{A}{b}$

where A/b is the drainage area per unit contour width (Fig. 3). Assuming Darcian flow parallel to the ground surface, M can be expressed as

[12] $\quad M = \dfrac{qA}{Tb\sin\theta}$

where θ is the head gradient driven by the ground surface slope. At the time of landsliding $M = M_c$ and higher values of M_c are used to estimate relative hydrologic response. For more detailed discussions of the model, its assumptions, and performance see Dietrich et al. (1993, 1995), Montgomery and Dietrich (1994), and Montgomery et al. (1998, 2000).

Through eqs. [10] and [12] the conditions necessary to trigger landsliding can be expressed as

[13] $\quad \left(\dfrac{q}{T}\right)_c = \dfrac{b\sin\theta}{A}\left[\dfrac{c_1 A_1 + c_b A_b}{A_b \rho_w gz\cos^2\theta\tan\phi'} + \dfrac{\rho_s}{\rho_w}\left(1 - \dfrac{\tan\theta}{\tan\phi'}\right)\right]$

where the ratio $(q/T)_c$ represents the critical magnitude of the apparent, steady-state rainfall, q, to the subsurface ability to convey water downslope, T. All else constant, the larger the value q relative to T, the more likely the hydrologic response will reach levels capable of inducing instability. As the hydrologic parameters of q and T are largely unconstrained and likely to vary considerably in both time and space, we opt to solve for the ratio $(q/T)_c$.

Study areas

Portions of the Oregon Coast Range are highly dissected with narrow ridgetops, steep slopes (32–47°), and local re-

lief typically less than 1000 m (Fig. 1). Landslides in shallow soil, and associated debris flows, can act as a primary sediment transport mechanism in the region (e.g., Burroughs and Thomas 1977; Pierson 1977; Dietrich and Dunne 1978; Swanson et al. 1981; Amaranthus et al. 1985; Robison et al. 1999). Furthermore, research indicates that many of these landslides occur during intense rainfall, mobilizing into debris flows (Pierson 1977; Montgomery et al. 1997). The Oregon Coast Range has also been the focus of intense industrial forestry, with accelerated landsliding after logging and road construction (Swanston and Swanson 1976; Swanson et al. 1977, 1981; Ketcheson and Froehlich 1978; Gresswell et al. 1979). Precipitation occurs mainly during the winter in this wet, mild, maritime climate, with mean annual totals between 1500 and 3000 mm (Corliss 1973).

Bedrock and soil properties

We examined 41 sites within the three study areas depicted by the open circles and asterisk in Fig. 1. All sites are underlain by arkosic, feldspathic, and micaceous rhythmically bedded sandstone with mudstone and siltstone interbeds of the Eocene Tyee or Flournoy formations (Dott 1966; Lovell 1969; Walker and MacLeod 1991). Many of the beds are graded, ranging from coarse sandstone at the base to fine sandstone and siltstone above. The colluvial soils derived from this bedrock are well-mixed, nonplastic, gravelly sands with sandstone clasts up to tens of centimetres in diameter. Laboratory tests reveal a nonplastic colluvial material with a mean Atterberg plastic limit of about 56% (Schmidt 1999). Stress path analyses of low confining stress triaxial strength tests (our own unpublished study of eight tests on five samples from two different sites) indicate the colluvium has a friction angle of $\phi' = 40°$ and is essentially cohesionless ($c_s' = 0$). Previously published values of internal friction angles for colluvial soils derived from the Tyee Formation vary from 35° to 44° (Yee and Harr 1977; Schroeder and Alto 1983; Burroughs 1985; Wu et al. 1988a). Consistent with Yee and Harr (1977), our triaxial strength tests indicate that the soil is essentially cohesionless ($c_s' = 0$). Continual mixing and downslope transport due to gravitational creep, intense bioturbation, and tree throw on the steep hillslopes preclude development of significant pedogenic structure and result in a colluvium that varies little in depth and space. The colluvial soil is mapped by Haagen (1989) as a very gravelly sandy loam at the surface to a cobbly loam at depth. Under the Unified Soil Classification System the soils are classified as GM.

Land ownership

The 41 sites are located on private, state, and federal land exhibiting a wide variety of management techniques and varying levels of anthropogenic disturbance. As a separate study, the Oregon Department of Forestry (ODF) initiated ground-based field studies to map and characterize more than 400 landslides surveyed over 50 square miles (130 km²) (Robison et al. 1999). We used the ODF maps to locate some of the same landslides to quantify root cohesion in various vegetation communities. We examined landslides occurring in November 1996 that were located northeast of Coos Bay in the Elliot State Forest (ESF), in private timber land northeast of Coos Bay, and in private timber lands northwest

Table 1. Twelve dominant and 16 associated species of coniferous, hardwood, and understory vegetation in the Oregon Coast Range.

Dominant species	Associated species
Coniferous	
Douglas-fir (*Pseudotsuga menziesii*)	Grand fir (*Abies grandis*)
Western hemlock (*Tsuga heterophylla*)	
Hardwood	
Oregon maple (*Acer macrophyllum*)	Big leaf maple (*Acer macrophyllum*), Douglas maple (*Acer glabrum*), cinquapin (*Castanopsis chrysophylla*), madrone (*Arbutus menziesii*)
Red alder (*Alnus rubra*)	Beaked hazelnut (*Corylus cornuta* var. *californica*), sitka willow (*Salix sitchensis*)
Vine maple (*Acer circinatum*)	Pacific rhododendron (*Rhododendron macrophyllum*)
Understory	
Blue elderberry (*Sambucus caerulea*)	
Foxglove (*Digitalis purpurea*)	
Himalayan blackberry (*Rubus discolor*)	Salmonberry (*Rubus spectabilis*), black raspberry (*Rubus leucodermis*), trailing blackberry (*Rubus ursinus*), black gooseberry (*Ribes lacustre*)
Dull Oregon grape (*Mahonia nervosa*)	Salal (*Gaultheria shallon*), kinnikinnick (*Arctostaphylos uva-ursi*)
Pearly everlasting (*Anaphalis margaritacea*)	
Sword fern (*Polystichum munitum*)	Piggy-back plant (*Tolmmiea menziesii*)
Thimbleberry (*Rubus parviflorus*)	Red huckleberry (*Vaccinium parvifolium*)

Note: See Fig. 5 for critical tensile force curves of the roots of the dominant species. Tensile force curves for associated species of vegetation are tied to that of the dominant species.

of Roseburg. Farther north in the Mapleton District, a composite of federal and private lands, we examined landslides triggered during storms in February 1996. We visited landslides within 7 months of each storm (some within 2 days of landsliding), prior to the decay of the small-diameter roots and degradation of the landslide scarps. Our aim was to sample sites containing common vegetation communities of the region.

Vegetation characteristics

The regional "Tsuga heterophylla" vegetation zone, extending from British Columbia south to the Klamath Mountains, delineates where vast stands of Douglas-fir (*Pseudotsuga menziesii*) and coastal western hemlock (*Tsuga heterophylla*) once occurred, and as such it is important to timber production (Franklin and Dyrness 1969). All the coniferous and most of the hardwood vegetation are characterized by a single upright trunk that branches in the upper part to form a crown. The understory vegetation can be dense with many well-branched stems within 2 m of the ground surface. In Table 1 we identify 12 dominant species of conifer, hardwood, and understory vegetation; we directly measured the strength of individual root threads of these species. Root strength regression curves for the additional 16 associated species of vegetation were correlated to the dominant species (shown in Table 1).

Within the larger Tsuga heterophylla zone, subsets of vegetation communities form in response to local growing conditions and land-use history. Our research quantifies root cohesion in a variety of vegetation communities with varying density, species composition, and health–condition in the regions noted in Fig. 1. We chose not to label land-use categories exclusively as a function of forest stand age because this label can belie a complicated history. In addition to the stand age of the dominant vegetation, we include the relative level of anthropogenic disturbance. Ten categories associated

with the style of measurement and local management-related activities were identified for the 41 study sites (Table 2): (1) pit in natural forest with trees ~300 years old ($n = 3$), (2) landslide in natural forest with trees ~200 years old ($n = 1$), (3) inferred natural forest root cohesion from stumps and roots of ~300-year-old trees surrounding landslide in 9.5-year-old clearcut ($n = 2$) (to infer the root cohesion of the natural forest, the decay function of eq. [14] is ignored; $t = 0$), (4) blowdown-induced landslide in natural forest with trees 200–300 years old ($n = 2$), (5) pit in industrial forest (ESF) with trees 100 years old in a forest that was commercially thinned approximately 30 years prior to measurement ($n = 2$), (6) landslide in industrial forest (ESF) ranging in age from 96 to 109 years old where sites experienced prior clear-cutting without subsequent planting ($n = 12$), (7) landslide in industrial forest (Mapleton) with trees ranging in age from 43 to 123 years old ($n = 2$) (the 43-year-old site was planted with fir seedlings after harvest, whereas the 123-year-old site was not replanted), (8) pit in clearcut ranging in age from 9 to 11 years ($n = 8$), (9) landslide in clearcut ranging in age from 6 to 9.5 years ($n = 8$), and (10) pit in herbicided clearcut <4 years old ($n = 3$). Sources for stand age include unpublished ODF data and unpublished data obtained during this study. All landslides are "in-unit" failures. That is, none are directly related to road drainage or mass wasting of engineered fill or sidecast along roads.

The natural or old-growth forest sites (categories 1–4) were selected to provide a spectrum of root cohesion within unharvested forests. Natural forests are dominated typically by Douglas-fir, western hemlock, vine maple (*Acer circinatum*), and sword fern (*Polystichum munitum*). Species surrounding the natural forest landslide of category 2 were dominated by vine maple with Douglas-fir and red alder (*Alnus rubra*). Unharvested, natural forest stands are assigned a 300-year age, as a stand-resetting fire occurred over much of the study area at this time. Root cohesion for sites

© 2001 NRC Canada

Table 2. Morphologic characteristics of landslides and pits with associated root attributes in different vegetation communities.

Basal area (m²)	Lateral area (m²)	Median depth (m)	Landslide perimeter (m)	Landslide volume (m³)	Slope (°)	No. of roots	Lateral root cohesion (kPa)	Tensile force (kg·m/s², ×10³)	Median root depth (m)	A/b (m)	A/b sin(slope) (m)	Time since disturbance (years)
Natural Forest Pit												
—	2.12	1.25	—	—	34	351	151.9	321.5	0.40	50	89	300
—	1.92	0.94	—	—	34	355	94.3	181.5	0.12	3482	6227	300
—	2.15	1.46	—	—	34	247	50.8	105.5	0.30	3122	5583	300
							94.3					
Natural Forest Landslide												
59.1	26.78	0.83	24.5	49.1	38	237	11.0	322.1	0.37	1250	2030	200
Inferred Natural Forest												
132.0	15.40	0.70	20.5	92.4	37	95	58.8	904.9	0.20	1171	1946	300
75.0	16.42	0.71	18.5	53.3	39	507	83.9	1377.1	0.15	2031	3227	300
							71.4					
Natural Forest Blowdown Landslide												
42.0	75.52	0.82	71.8	34.4	43	514	33.4	2524.1	0.38	43	63	200
30.9	17.81	0.58	27.6	17.9	39	656	17.8	316.4	0.20	140	222	300
							25.6					
Industrial Forest Pit												
—	3.46	1.30	—	—	32	425	36.5	85.9	0.40	798	1506	100 (30)
—	2.74	0.88	—	—	35	96	9.8	24.9	0.20	570	994	100 (30)
							23.2					
Industrial Forest Landslide												
Elliot State Forest (ESF)												
72.2	21.75	1.07	22.5	77.3	44	100	4.2	90.5	0.10	22	32	109
31.6	13.07	0.74	15.2	23.4	46	780	3.8	49.3	0.15	125	174	103
7.4	1.29	0.16	8.8	1.2	44	947	2.2	2.9	0.15	111	160	103
14.4	4.31	0.48	12.7	6.9	47	628	2.8	12.0	0.15	104	142	103
34.0	27.40	1.64	18.0	55.8	40	536	12.1	330.3	0.20	244	379	96
44.9	26.96	1.19	17.7	53.4	43	1291	8.3	222.4	0.10	500	733	96
—	6.61	0.67	—	—	43	355	1.8	12.2	0.10	500	733	96
—	5.54	1.28	—	—	43	138	10.9	60.2	0.05	500	733	96
11.4	11.30	1.02	11.0	11.7	45	2207	6.9	78.2	0.10	1029	1455	103
5.6	3.23	0.62	4.9	3.5	34	1050	8.8	28.6	0.10	1596	2854	103
40.2	31.27	1.09	25.4	43.8	32	563	3.5	108.2	0.10	1596	3012	100
							6.8					
Cut-boundary												
179.2	19.44	0.51	45.8	91.4	42	2922	8.9	183.1	0.20	20	30	109
Mapleton District												
35.8	14.29	0.65	17.3	23.2	44	245	21.3	304.1	0.38	222	320	43
51.3	21.86	0.72	24.5	36.9	43	617	6.6	144.5	0.28	233	342	123

Table 2 (*concluded*).

Basal area (m²)	Lateral area (m²)	Median depth (m)	Landslide perimeter (m)	Landslide volume (m³)	Slope (°)	No. of roots	Lateral root cohesion (kPa)	Tensile force (kg·m/s², ×10³)	Median root depth (m)	A/b (m)	A/b sin(slope) (m)	Time since disturbance (years)
Clear-cut Pit												
—	0.73	0.73	—	—	34	20	1.3	0.9	—	118	212	9
—	0.50	0.50	—	—	44	20	2.6	1.3	—	88	127	9
—	0.69	0.69	—	—	38	47	3.1	2.1	—	48	78	9
—	1.10	1.10	—	—	45	50	5.0	5.5	—	197	279	9
—	2.58	1.23	—	—	41	123	9.4	0.9	0.30	256	390	11
—	1.98	0.94	—	—	40	124	8.3	16.5	0.15	634	986	11
—	1.85	0.82	—	—	46	106	10.0	18.4	0.10	382	531	11
—	1.71	0.69	—	—	39	109	10.5	18.0	0.15	300	477	11
							6.7					
Clear-cut Landslide												
139.4	53.28	2.04	41.00	284.3	44	104	0.3	15.9	0.80	354	510	6
210.0	63.34	1.10	50.00	231.0	39	280	1.7	105.1	0.60	423	672	6
65.0	43.90	1.18	30.30	76.8	44	206	1.3	57.2	0.32	288	414	9
105.9	63.42	1.01	44.50	106.9	45	345	2.0	127.7	0.45	1220	1726	7
98.0	20.79	0.94	37.00	92.1	44	363	4.6	95.0	0.30	464	668	9
135.3	34.40	0.80	43.30	108.2	42	1063	3.4	116.8	0.25	390	583	9
132.0	15.40	0.70	20.50	92.4	37	1961	7.3	74.2	0.20	1171	1946	9.5
75.0	16.42	0.71	18.50	53.3	39	900	9.8	81.7	0.15	2031	3227	9.5
							2.7					
Herbicided Clear-cut Pit												
—	1.27	0.66	—	—	38	177	1.5	1.1	0.06	398	646	<4
—	1.59	0.76	—	—	43	74	2.1	2.5	0.05	133	194	<4
—	1.31	0.98	—	—	43	77	0.9	0.9	0.20	765	1121	<4
							1.5					

Note: Values in bold at the base of individual vegetation communities represent median value of root cohesion for land-use type. Values for time since disturbance of industrial forest pits represent clear-cutting, with values for thinning in parentheses.

Table 3. Quantity and size of hardwood (red alder and Oregon maple) and coniferous (Douglas-fir and western hemlock) trees within 12 m surrounding landslide scarps in the Mapleton District ($n = 21$) and Elliot State Forest ($n = 12$).

	Hardwood		Coniferous		
	Live	Dead	Live	Dead	Stumps
No. of trees per landslide					
Mapleton District	6.7	0.2	1.1	0.7	0
Elliot State Forest	2.8	0.1	3.5	0.8	0.8
Mean diameter at breast height of trees (± standard deviation; m)					
Mapleton District	0.21±0.17	0.33±0.10	0.81±0.49	0.88±0.43	na
Elliot State Forest	0.16±0.15	0.40	0.63±0.37	0.88±0.40	0.97±0.29

Note: na, not available.

within category 3 was calculated based upon the diameters of roots associated with old-growth coniferous stumps identified in the field, as if the roots were alive. Although some of the smaller diameter roots may have completely decayed in the 9.5 years since cutting, the recognition of roots emanating from stumps provides a means to infer root cohesion at the time of harvesting. In category 4, areas of blowdown in natural forests represent sites where a lever-arm influence from the length of falling tree augments the hydrologic response to induce landsliding. The wind pressure on trees generated by the bulk aerodynamic resistance of vegetation is not considered in our slope stability analyses. The diameter at breast height of Douglas-fir trees within categories 1 and 4 typically ranges between 0.5 and 1.5 m.

We use the term industrial forest (categories 5–7) to denote commercially harvested stands of trees in the Mapleton District and Elliot State Forest. These stands are significantly influenced by land management such as previous timber harvesting, commercial thinning, or intentional use of fire (much of the vicinity was burned in the late 19th Century to flush game and clear land). Industrial forests consist of a mosaic of conifers (Douglas-fir and western hemlock), hardwoods (Oregon maple (*Acer macrophyllum*) and red alder), and understory vegetation. The pits representing category 5 were located in an area that was clear-cut 100 years prior and commercially thinned about 30 years prior to the measurement of root cohesion. Within categories 6 and 7, landslides in the commercial lands of the Mapleton District and Elliot State Forest, the mean number of live hardwood trees (primarily red alder and Oregon maple) within 12 m surrounding a landslide scarp exceeded that of live coniferous trees (Douglas-fir and western hemlock) (Table 3). The mean number of nearby (i.e., ≤12 m radius) live hardwoods ranged between roughly 3 and 7 trees per landslide, whereas the number of live coniferous trees was only 1–3.5 trees per landslide. The diameter at breast height of live conifers (0.63–0.81 m), though, exceeded that of live hardwoods (0.16–0.21 m) for both sites. The relative lack of coniferous vegetation and dominance of hardwood vegetation in industrial forests was distinctive for sites harvested up to 100 years prior to the measurement of root cohesion.

Recently established vegetation in clearcuts less than 11 years old (categories 8 and 9) was distinguished by an abundance of understory vegetation, red alder, and planted conifer seedlings. The sites in category 10 (herbicided clear-cut pits) were clear-cut harvested and treated with herbicides to halt the growth of understory vegetation less than 4 years prior to the root cohesion measurements. Vegetation was dominated by planted saplings of Douglas-fir, pearly everlasting (*Anaphalis margaritacea*), Himalayan blackberry (*Rubus discolor*), and sword fern.

Methods

Site characterization

In the field we examined landslide source volumes triggered by storms in 1996, areas of wind-induced blowdown, and hand-dug pits with vertical exposures greater than 1 m^2 extending to the colluvium–bedrock interface. Hand-dug pits were selected in steep, hillslope hollows (areas of topographic convergence) filled with colluvium, as they represent potential initiation sites of shallow landslides. Tree and stump spacing was measured with a fiberglass tape, and pits were dug midway between neighboring trees or stumps. Ground surface slope, θ, was measured over the length of the landslide or hillslope hollow using hand-held clinometers. Similarly, the ratio A/b was determined from field measurements rather than from digital elevation models. The upslope contributing area, A, was measured with a laser rangefinder and (or) fiberglass tapes and was defined based upon local drainage divides visible from the ground surface such as interfluves and ridge tops. The contour width through which the subsurface discharge flows, b, was represented by the width of the landslide scarp.

Root cohesion calculation

Root cohesion, c_r, was estimated by calculating the root area ratio, A_r/A_s, and root-thread strength, T_r, for separate species of vegetation. To calculate the root cohesion specific to individual species, we carried out tensile strength tests for thread diameters up to 6.5 mm for 12 species of vegetation characteristic of the field area (Table 1). We trimmed 15–20 cm long root segments from the plant, measured diameters including bark, clamped one end of the roots to a calibrated spring, and loaded roots to failure in tension similar to the procedure described in Wu et al. (1979). The load registered on the spring at failure determined the maximum tensile force provided by the root. Regression curves of the thread strength versus root diameter data were subsequently used to extrapolate root tensile strength for threads >6.5 mm in diameter.

Fig. 4. Photograph of broken roots (highlighted) in landslide scarp within Elliot State Forest. Roots did not simply pull out of soil matrix, but broke during the landslide. Note 2 m tall person for scale in center (in center of annotated circle) and absence of roots on the basal surface of the landslide.

We measured characteristics of all roots with diameters ≥ 1 mm in regions with differing vegetation communities. Field-measured root attributes included species, diameter (measured with micrometer), vertical depth relative to the ground surface, whether the root was alive or decaying, whether the root was broken or intact, and cross-sectional area of colluvium over which roots act. The root attribute inventory was divided into polygons of similar soil depth with a typical length of about 2 m along the landslide scarps. Root cohesion for each polygon was calculated separately and the spatially weighted mean was used to represent a single value of root cohesion for a site.

Live and decaying roots were identified based on their color, texture, plasticity, adherence of bark to woody material, and compressibility. For example, live Douglas-fir roots have a crimson-colored inner bark, darkening to a brownish red in dead Douglas-fir roots. Both are distinctive colors. Live roots exhibited plastic responses to bending and strong adherence of bark, whereas dead roots displayed brittle behavior with bending and poor adherence of bark to the underlying woody material. We measured the tensile strength of decaying root threads within clearcuts and found that their tensile strength was significantly lower than their ultimate living tensile strength. We assumed that all dead roots in forested areas (both natural and industrial) and dead

understory roots in clearcuts had no root cohesion because we do not know the timing of plant mortality and hence the relative decrease in thread strength. Consequently, calculated root cohesion is conservative on the low side because decaying roots continue to contribute a finite amount of cohesion. We did not systematically characterize the decay function of all the species in the area. Instead we uniformly characterize the tensile strength decrease over time of all conifer roots (living and decaying) with the coast Douglas-fir decay function defined by Burroughs and Thomas (1977), such that
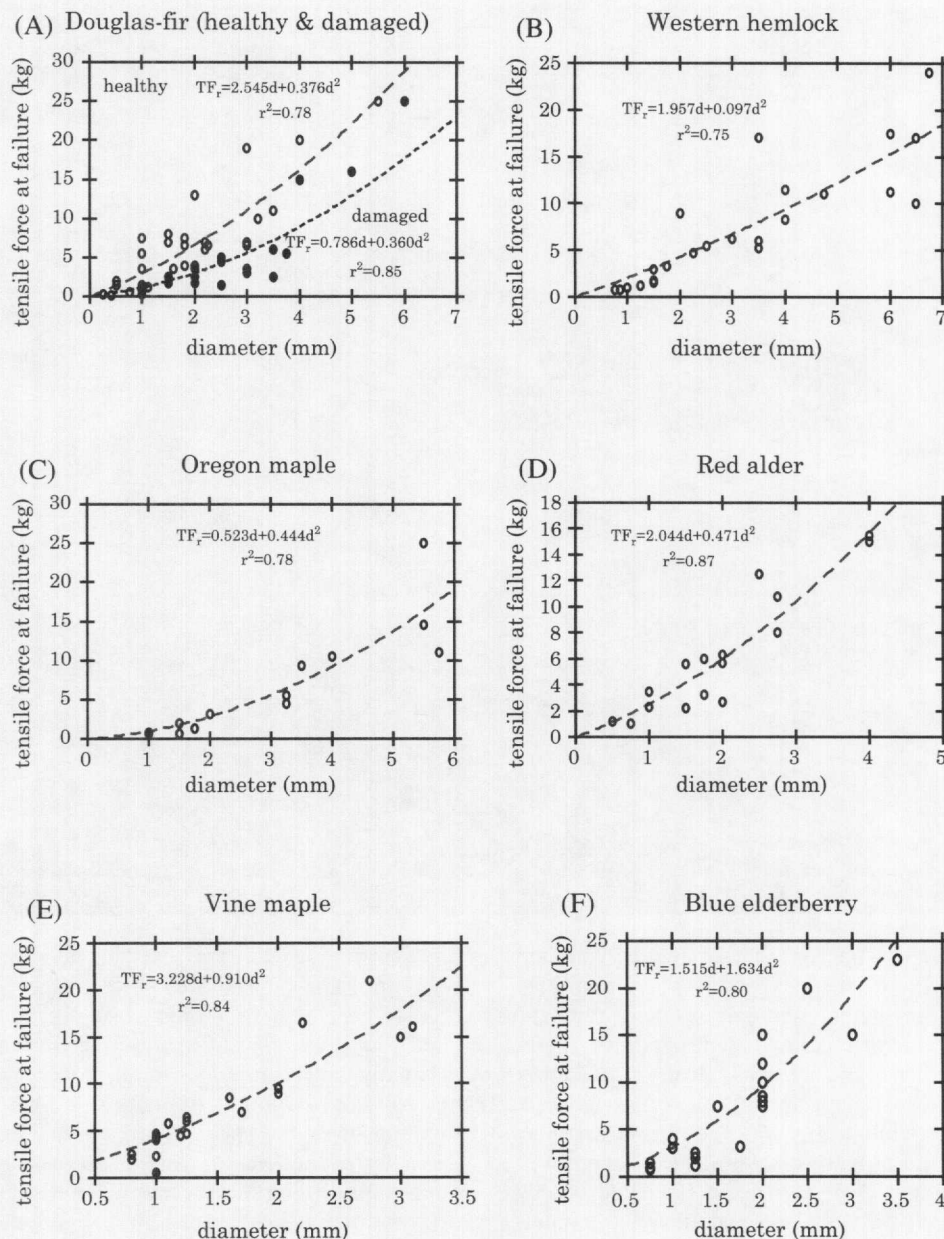
$$[14] \quad TF_r = 1.04(2.516 d_{wb})^{1.8 - 0.06\sqrt{t}}$$

where d_{wb} is the root-thread diameter (mm) without bark, t is the time since timber harvest (months), and TF_r is expressed in kilograms. Live root tensile strength is calculated with $t = 0$. Burroughs and Thomas determined eq. [14] by breaking roots in tension up to 14.3 mm in diameter (without bark) using a hydraulic-pressure device to anchor the root ends.

Results

Field observations illustrate that root networks of the 12 dominant species (Table 1) varied from fine fibrous systems

Fig. 5. Critical tensile force of individual root threads of varying diameter for the 12 primary species of vegetation (Table 1). Note significant decrease in tensile force for live roots of Douglas-fir trees in the ESF damaged in thinning operation during the 1960s (solid circles).
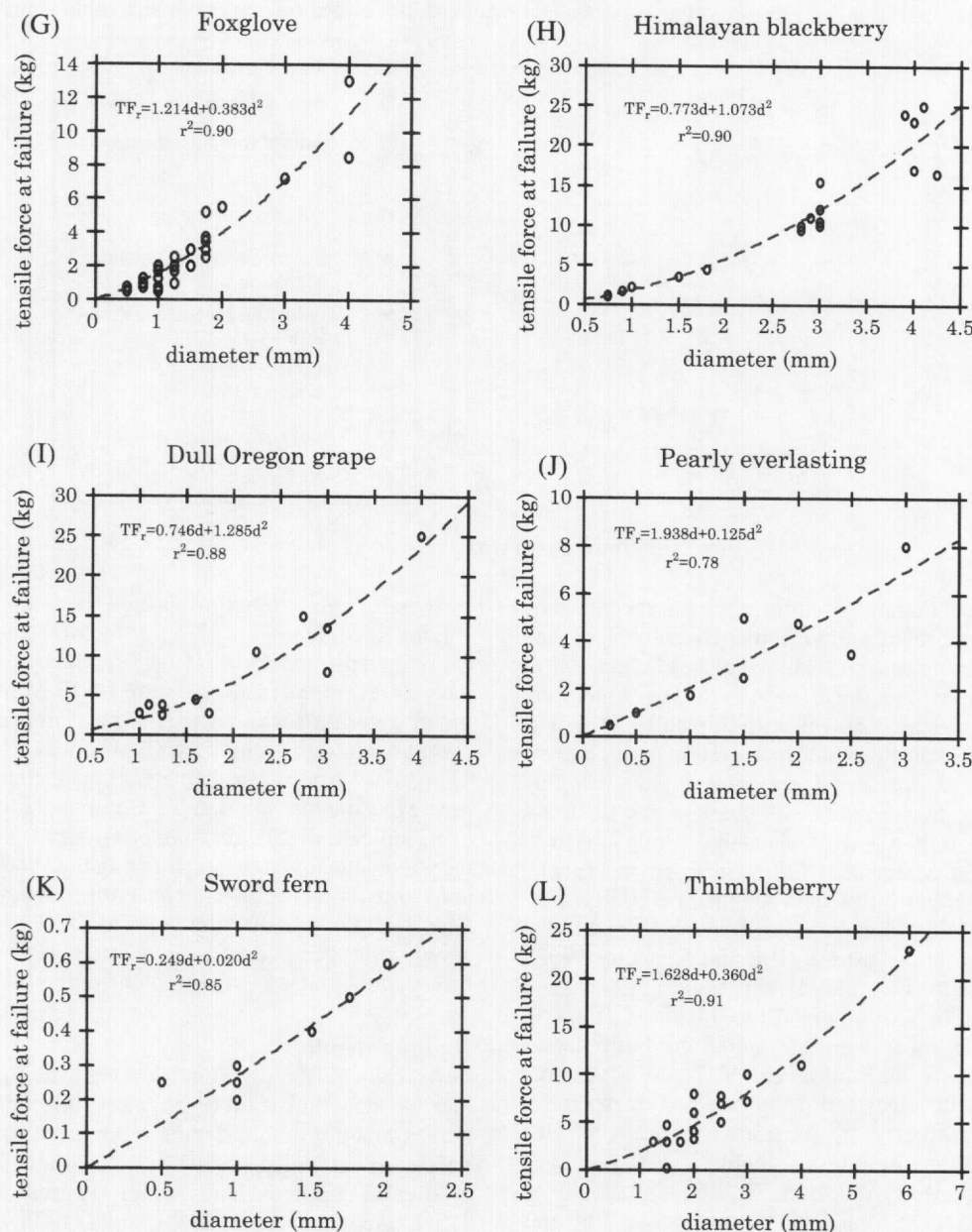

through intricate branched systems and growth habits of trees and understory vegetation were highly variable, even within one species growing in different environments. The majority of roots emanating from landslide scarps were oriented roughly parallel to the ground surface within the colluvium. In response to the steep topographic gradients, roots appear to preferentially grow upslope, oriented opposite to the greatest downslope component of gravity. The associated tensile stresses may stimulate roots to thicken in the upslope direction and function as anchors. Large, vertical taproots extending downward into saprolite and fractured bedrock were uncommon, most likely because in moist soils with high groundwater levels roots tend to spread laterally, forming plate-like or disk-like root masses. The colluvial soil de-

posits of the landslides examined were sufficiently thick that the bulk of the roots did not penetrate into the bedrock and the occurrence of roots on the basal area of the landslides was uncommon.

We noted a preponderance of exposed, blunt stubs of broken roots in the margins of recent landslide scarps (Fig. 4), solid evidence that roots broke prior to pulling out of the soil matrix (also identified by Wu 1976 and Gray and Leiser 1982). Roots terminating in blunt ends often protruded up to tens of centimetres from the scarp. Roots were not straight and smooth, but rather exhibited tortuous growth paths with a firmly anchored, interlocking structure. Wu et al. (1988b) concluded that resistance of relatively weak soil is insufficient to prevent roots from straightening out during soil
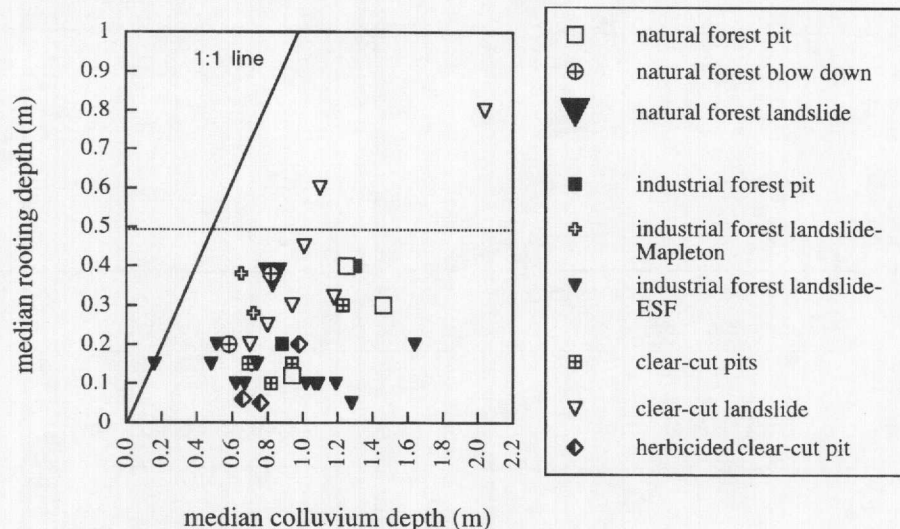
Fig. 5 (*concluded*).

(G) Foxglove
$TF_r = 1.214d + 0.383d^2$
$r^2 = 0.90$

(H) Himalayan blackberry
$TF_r = 0.773d + 1.073d^2$
$r^2 = 0.90$

(I) Dull Oregon grape
$TF_r = 0.746d + 1.285d^2$
$r^2 = 0.88$

(J) Pearly everlasting
$TF_r = 1.938d + 0.125d^2$
$r^2 = 0.78$

(K) Sword fern
$TF_r = 0.249d + 0.020d^2$
$r^2 = 0.85$

(L) Thimbleberry
$TF_r = 1.628d + 0.360d^2$
$r^2 = 0.91$

shear at shallow depths. Therefore, root threads with high tortuosities will straighten prior to breaking and can result in a length of root jutting out from the scarp toward the evacuated landslide source volume. Similarly, broken roots may be concealed within the mass of remaining colluvium, making them difficult to identify without substantial excavation. Furthermore, longer roots mobilize their maximum tensile strength at higher displacements than shorter roots because pullout resistance increases with root length until the breaking strength of the root is reached (eq. [6]). In the runout path of the debris flows originating from the landslides, however, we noted that root tendrils were extremely abraded by the passage of debris but remained intact, displaying the entire branched network of roots including fine fibers <1 mm in diameter. Hence roots outside of the landslide source volume attest to an evacuation of soil from around

the root network or a pulling out of the roots from the soil matrix.

Species variation of tensile root force

We generated 12 tensile force curves characterizing both the primary and secondary vegetation (Table 1; Fig. 5) in the study area. The tensile force of root threads at failure increases with an increase in diameter such that second-order polynomial regression curves ($TF_r = jd + kd^2$) fit the data well. In Fig. 5, regressions are plotted as broken lines with associated regression coefficients, r; TF_r is expressed in kilograms, d is the root-thread diameter with outer bark (mm), and j and k are constants specific to a given species. Measurement of root length before and after strength testing reveals that plastic deformation prior to brittle failure produced strains of roughly 5–10%. In addition to root di-

Fig. 6. Median rooting depth versus median colluvium depth for different land-use types and vegetation communities. The broken line represents rooting depth of 0.5 m, and the solid line a one-to-one relationship between rooting depth and colluvium depth.
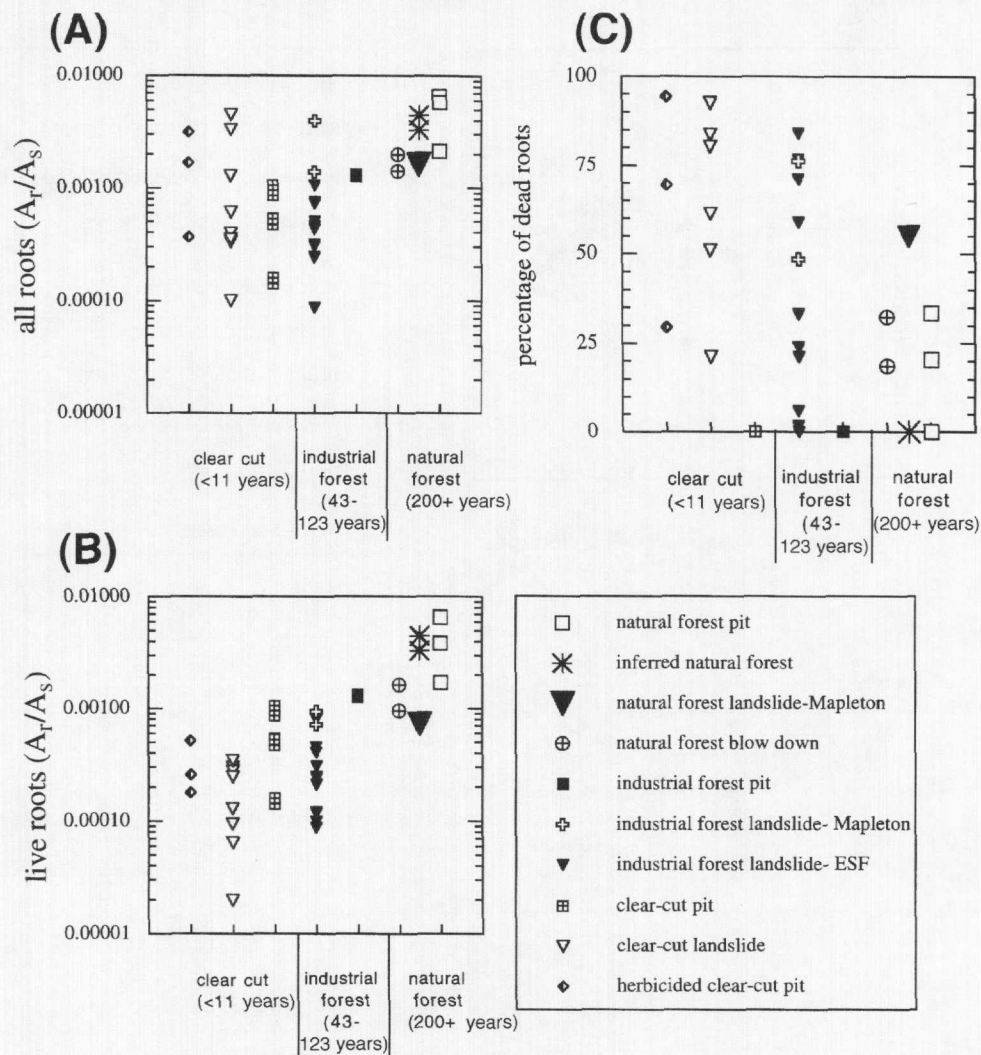

ameter, tensile force variation within a given species may arise from different growing environments (Burroughs and Thomas 1977), growing season (Hathaway and Penny 1975), or root orientation, where those roots growing uphill are stronger than those oriented downhill (Schietchtl 1980). The observed lateral roots of plate-like root systems which grow close to the ground surface experience higher bending stresses than highly tapered roots of heart or tap systems, and as a result the root wood of plate-like root systems is stronger (Stokes and Mattheck 1996). These environmental factors engender changes in tracheid length, specific gravity, fibril angle, and cellulose content, all influencing the amount of material resisting applied stress (Ifju and Kennedy 1962). Environmental variations are clearly expressed in the case of Douglas-fir subject to varying land-use histories (Fig. 5). Healthy Douglas-fir roots were measured in both unharvested, natural forests and in areas of 7- to 8-year-old planted seedlings after clear felling (plotted as open circles in Fig. 5). Alternatively, in portions of the ESF the yarding-cable, thinning operations in the 1960s damaged tree canopies and scarred trunk bark. Subsequent fungal infestation appears to have weakened the trees, and the roots chronicle this disturbance with lower thread strengths. Because we do not know the spatial extent of the damaged roots resulting from this thinning operation, we carried out all subsequent analyses using the ultimate (healthy) root tensile strength. The tensile root strength data for Douglas-fir and western hemlock shown in Fig. 5 are for comparative purposes only. They were not used in the subsequent calculations of the root cohesion contribution from coniferous species. Rather, we used the root tensile strength function (eq. [14]) reported in Burroughs and Thomas (1977) for all coniferous roots because (*i*) the roots tested were of larger diameter, and (*ii*) a decay function was estimated. Higher root-thread tensile forces result from using eq. [14] instead of the functions reported in Fig. 5. Root cohesion estimates for all hardwood and understory species are calculated from the equations of tensile force at failure represented in Fig. 5.

Tensile root strength reported here concurs with other studies specific to the Oregon Coast Range. For example, Commandeur and Pyles (1991) report that Douglas-fir roots have an average tensile strength of 17 MPa (tensile load divided by cross-sectional area for a 3 mm diameter root). In comparison, our strength curve produces a tensile strength of 15.3 MPa for a 3 mm diameter thread. Estimated by laboratory experiments, the data of Commandeur and Pyles, however, indicate that larger diameter roots are stronger than our data indicate. In addition, Burroughs (1985) reports the root cohesion representative of an entire sword fern plant averages 1.7 kPa, whereas the cohesion is 2 kPa using our measured average density of sword fern roots (650 1 mm threads/m^2) and an average plant radius of 0.5 m.

Rooting depth

As root attribute inventories were divided into polygons along a landslide scarp or pit walls, the characteristic rooting depths and colluvium depths reported in Table 2 are median values of all polygons at a site. Although the majority of colluvium depths in landslide-prone areas range from 0.5 to 1.5 m, median rooting depths appear to be constrained to the upper 0.5 m of regolith (Fig. 6; Table 2). Root depth representative of a site in Fig. 6 was determined by calculating the median of all roots both live and decaying. Similarly, roots of deciduous trees in the eastern United States typically extend to depths up to 0.5 m (Stout 1956; Kochenderfer 1973; Riestenberg 1987). The fact that most roots are located within the upper 0.5 m of colluvium highlights the lack of tap roots or deeply penetrating roots in the Oregon Coast Range and reinforces the need to incorporate the lateral reinforcement arising from roots in slope stability analyses. The sites with the median rooting depths >0.5 m are not located in mature forests, but rather in clearcuts dominated by thimbleberry (*Rubus parviflorus*), vine maple, and Oregon maple. Maximum colluvium thickness in the region typically ranges from <0.5 m on topographic noses to <3 m in hollows (Pierson 1977; Dietrich and Dunne 1978; Montgomery et al. 1997; Schmidt 1999).

Fig. 7. Root area ratios (A_r/A_s) and percentage of dead roots for different vegetation communities. (A) Semilogarithmic plot reveals the density of roots, both live and decaying, is similar between most communities, with all communities expressing values $>10^{-3}$. (B) Root area ratios of only live roots are greatly reduced, indicating a significant fraction of decaying roots in clear-cut and industrial forest sites. (C) Percentage of dead roots [(root area ratio of dead roots)/(total root area ratio) × 100] for different vegetation communities.

Root area ratio and vegetation community

The root area ratio (A_r/A_s in eqs. [3] and [5]) provides a measure of root density within the colluvium. An examination of all the roots, both live and decaying, reveals that the different land-use types, and associated vegetation communities, share common values of A_r/A_s ranging from 10^{-4} to 10^{-2} (Fig. 7A). That is, considering all roots regardless of condition, sites within clearcuts and industrial forests have maximum root densities similar to those of natural forests. This range of root area ratios is consistent with values determined in other regions (Riestenberg 1994; Wu 1995). In contrast, if only the proportion of live roots is considered, the values of A_r/A_s for clear-cut and industrial forests markedly drop below 10^{-3} (Fig. 7B). Values of A_r/A_s for natural forests, however, remain largely above 10^{-3}. Laboratory experiments by Shewbridge and Sitar (1990) on the reinforcement properties and shear zone width (Fig. 2) indicate that the shear zone markedly in-

creases where reinforcement densities (A_r/A_s) exceed 10^{-2}. Furthermore, Shewbridge and Sitar conclude that the strength of densely reinforced soil is not linearly related to reinforcement concentration.

The significant reduction in values of A_r/A_s for live roots in the clear-cut landslide category indicates a large fraction of decaying roots. Fittingly, the largest percentage of decaying roots (up to 95%) are present in the categories of the herbicided clear-cut pit, clear-cut landslide, and industrial forest landslide categories (Fig. 7C). As the vast majority of decaying roots in herbicided clear-cut pits and clear-cut landslides are directly linked to nearby stumps, anthropogenic influences can serve to actively decrease the density of live root biomass. In contrast, the cross-sectional area of dead roots in natural forest pits and blowdown sites is limited to less than a third of the total area occupied by all roots, whereas the natural forest landslide is composed of about 55% dead roots.

Fig. 8. Lateral root cohesion values for different vegetation communities (each point represents one row in Table 2). (A) Semilogarithmic plot of lateral root cohesion depicts the distribution of all 41 sites ranges over three orders of magnitude. (B) Box plot showing median and quartiles for clearcuts, industrial forests, and natural forest sites.

Root cohesion and vegetation community

Figure 8 depicts the lateral root cohesion determined from up to thousands of roots per site (Table 2) in different vegetation communities growing under variable conditions. All values reported were calculated using eq. [5] along the lateral boundaries of a landslide or pit. Significant basal root cohesion >0.05 kPa in landslide scars was only observed at three sites. Basal cohesion measured within landslides ranged from 0.07 to 3.8 kPa, values equivalent to a small fraction of the lateral cohesion. Clear differences in lateral root cohesion emerge between the 10 categories in Table 2 and Fig. 8A. For instance, lateral root cohesion of herbicided

Table 4. Select published values of root cohesion for different species of vegetation obtained by measuring root diameters and strength, direct shear tests in forest soils, and back-calculation.

Root cohesion (kPa)	Vegetation type	Location	Source
Measurement of root diameter and thread strength			
3.5–7.0*	Sphagnum moss	Alaska	Wu 1984a
5.6–12.6*	Hemlock, sitka spruce, yellow cedar	Alaska	Wu 1984b
5.7[†]	Sugar maple	Ohio	Riestenberg and Sovonick-Dunford 1983
6.2–7.0*	Sugar maple	Ohio	Riestenberg and Sovonick-Dunford 1983
5.9*	Alaska cedar, hemlock, spruce	Alaska	Wu et al. 1979
7.5–17.5*	Douglas-fir	Oregon	Burroughs and Thomas 1977
In situ direct shear test			
1.0–5.0[†]	Japanese cedar	Japan	Abe and Iwamoto 1986
2.0–12.0[†]	Alder nursery	Japan	Endo and Tsuruta 1969
3.0–21.0[†]	Lodgepole pine	California	Ziemer 1981
3.7–6.4[†]	54-month-old yellow pine	Laboratory	Waldron et al. 1983
~5[†]	52-month-old yellow pine	Laboratory	Waldron and Dakessian 1981
6.6[†]	Beech	New Zealand	O'Loughlin and Ziemer 1982
Back-calculation			
1.6–2.1[†]	Grasses, sedges, shrubs, sword fern		
2.6–3.0[†]	Red alder, hemlock, Douglas-fir, cedar	Washington State	Buchanan and Savigny 1990
2.02[†]	Blueberry, devil's club	Alaska	Sidle and Swanston 1982
2.8–6.2[†]	Ponderosa pine, Douglas-fir, Engelmann spruce	Idaho	Gray and Megahan 1981
3.4–4.4[†]	Hemlock, spruce	Alaska	Swanston 1970

*Root cohesion representing lateral reinforcement.
[†]Root cohesion representing basal reinforcement.

slopes in recent clearcuts is well below 3 kPa, over an order of magnitude lower than values for natural forests which can exceed 100 kPa. The disturbance of understory vegetation during clear-cutting and subsequent application of herbicide appear to suppress available root cohesion. Although significant overlap in lateral root cohesion exists between sites in clearcuts and industrial forests, the median of natural forest sites is distinctly separated from clear-cut and industrial forest sites (Fig. 8B). In Fig. 8B each box encloses 50% of the data, with the median value of the variable displayed as a horizontal line, and the top (upper quartile, UQ) and bottom of the box (lower quartile, LQ) mark the interquartile distance (IQD) of the variable population. The vertical lines extending from the top and bottom of the box mark the minimum and maximum values within the data set that fall within an acceptable range (greater than UQ + 1.5 × IQD or less than LQ – 1.5 × IQD). Values outside of the acceptable range are plotted as open circles. Lateral root cohesion within natural and industrial forests differs substantially, with median values separated by up to an order of magnitude and little overlap between the populations (Fig. 8B; Table 2). The representative lateral root cohesion for blowdown-induced landslides in natural forests (median 25.6 kPa) is relatively lower than values for the natural forest pits; blowdown-induced landslides may preferentially occur in areas of lower than average lateral root cohesion. As the blowdown sites are located on the low end of the lateral root cohesion distribution of natural forests, it may be that the trees are weak or distressed and hence may selectively fall over during high winds.

Variation between lateral root cohesion populations in different land-use categories was defined using a variety of statistical techniques. Multiple comparisons using the Student t test revealed that mean values for each land-use type are statistically distinct (confidence level $\alpha = 0.05$); the industrial forest and clear-cut sites are more closely related than the natural forest sites are to either the clear-cut or industrial forest sites. As the lateral root cohesion data are not normally distributed, the nonparametric two-sample Kolmogorov–Smirnov test is applied to examine the null hypothesis that the two distributions are the same under the assumption that the two distributions are independent of each other (e.g., Press et al. 1992). Although the populations are small, the Kolmogorov–Smirnov test rejects the null hypothesis that the natural and industrial forest sites are drawn from the same root cohesion distribution ($\alpha = 0.05$). Thus the lateral root cohesion values for the natural and industrial forest sites come from distributions that have different cumulative distribution functions. In addition, the Kolmogorov–Smirnov test cannot reject the null hypothesis, indicating that the clear-cut and industrial forests could be part of the same distribution. Although lateral root cohesion in the natural forest sites is statistically distinct, the clear-cut and industrial forest sites are statistically similar.

Lateral root cohesion values reported here are similar to published values, except for those from the natural forest sites which are considerably higher (median 94.3 kPa) (Tables 2, 4). Burroughs and Thomas (1977) document a range of lateral root cohesion between 7.5 and 17.5 kPa, limited to roots less than 10 mm in diameter. Lateral root cohesion val-

© 2001 NRC Canada

Fig. 9. Box plots showing median and quartiles of broken and unbroken live roots within landslide scarps of clearcuts, industrial forests, and natural forests. Maximum outliers are 62 mm for clear-cut landslide unbroken roots, 61 mm for industrial forest (ESF) broken roots, 37 mm for industrial forest (ESF) unbroken roots, 53 mm for industrial forest (Mapleton) broken roots, 125 mm for natural forest blowdown broken roots, 110 mm for natural forest blowdown unbroken roots, and 87 mm for natural forest landslide broken roots. The median, upper quartile, and lower quartile diameters for the industrial forest (ESF) broken roots are all 1 mm.

Fig. 10. Lateral root cohesion of individual polygons along the perimeter of landslide source volumes. General age (in years) of vegetation is shown in parentheses after category title. Maximum outliers exceed 100 kPa for both natural forest blowdown and inferred natural forest sites.

ues from Burroughs and Thomas may be lower than the actual root cohesion provided by all vegetation because they limited their investigation to roots <10 mm in diameter and they neglected the roots of hardwood and understory vegetation. Nevertheless, their lateral root cohesion values remain higher than our median root cohesion representative of industrial forests.

Lateral root cohesion in old-growth, natural forests pits may overestimate reinforcement because we assume the breaking strength, T_{ri}, is less than the pull-out resistance, F_p, of the soil–root bond. Although measurements in scarps include only those roots broken by the landslide, root cohesion estimates in pits include all roots intersecting the plane of the pit wall. For large-diameter roots, though, the thread strength may exceed the resistance of the soil–root bond (Stolzy and Barley 1968; Waldron and Dakessian 1981), allowing the intact root to pull through the soil matrix and precluding the mobilization of the full root strength in the event of a landslide. For comparative purposes, if we assume thread strengths of roots >10 mm in diameter (the range of root diameters examined in Burroughs and Thomas 1977) exceed the soil–root resistance, we limit the contribution of root cohesion to the smaller size fraction of roots where F_p is more likely to exceed T_{ri}. Limiting the contribution of root cohesion to the size class of roots <10 mm in diameter decreases root cohesion in the undisturbed forest pits from 151.9 to 21.1 kPa, from 94.3 to 27.0 kPa, and from 50.8 to 23.7 kPa. Even with the imposed diameter bound, values for natural forests (median 23.7 kPa) remain higher than those reported in Burroughs and Thomas (1977) and all of the industrial forest landslide sites. In addition, by excluding the influence of roots >10 mm in diameter, we underestimate reinforcement because when larger diameter roots slip through

Fig. 11. Variation in measured landslide source volumes with land-use type and general vegetation age revealing greater volumes for clear-cut landslides. Spatially uniform, lower root cohesion values (Fig. 10) may allow for larger landslides in clearcuts.

the soil they still contribute a reinforcing increment (Waldron and Dakessian 1981). We infer that complex load transfers may occur such that the last resistance to movement is the displacement between soil and large-diameter roots. During landslide initiation, larger diameter roots may share the imposed load with the smaller diameter roots until the smaller diameter roots break, at which time soil may slip along the large-diameter roots. This does not preclude equivalent tensile forces applied to roots of large diameter and a contribution to the total lateral root cohesion.

Root diameter and soil–root bond

To estimate the influence of the soil–root bond relative to the root-thread strength, we noted the diameters of broken and unbroken live roots in landslide scarps. In the following analysis dead roots were not included because they are relatively weak for their diameter. Figure 9 reveals that the live, unbroken roots generally have greater diameters than broken roots for landslide scarps in all land-use types. The largest range in root diameter, for both broken and unbroken roots, was found at the blowdown sites. Although broken roots vary greatly in their diameter (numerous outliers in Fig. 9; box plot characteristics are the same as those for Fig. 8B), the median values are consistently lower than those for the unbroken roots. We observed large-diameter broken roots; maximum diameters of live broken roots is 122 mm for Douglas-fir, 87 mm for vine maple, 69 mm for western hemlock, and 42 mm for red alder. It is possible that these large-diameter roots were aligned parallel to the direction of maximum tensile force, received the largest load, and broke before other smaller diameter roots. The percentage of unbroken roots relative to the total number of roots is also diagnostic. In landslide scarps the percentage of unbroken roots is 2.5% in clearcuts, 1.7% in the ESF industrial forests, 14.0% in the Mapleton industrial forests, 3.9% in natural forest blowdowns, and 20.2% in natural forests. The general relationship that unbroken roots are consistently greater in diameter and less numerous than broken roots lends cre-

dence to the assertion that larger diameter roots tend to slip through the soil matrix without breaking.
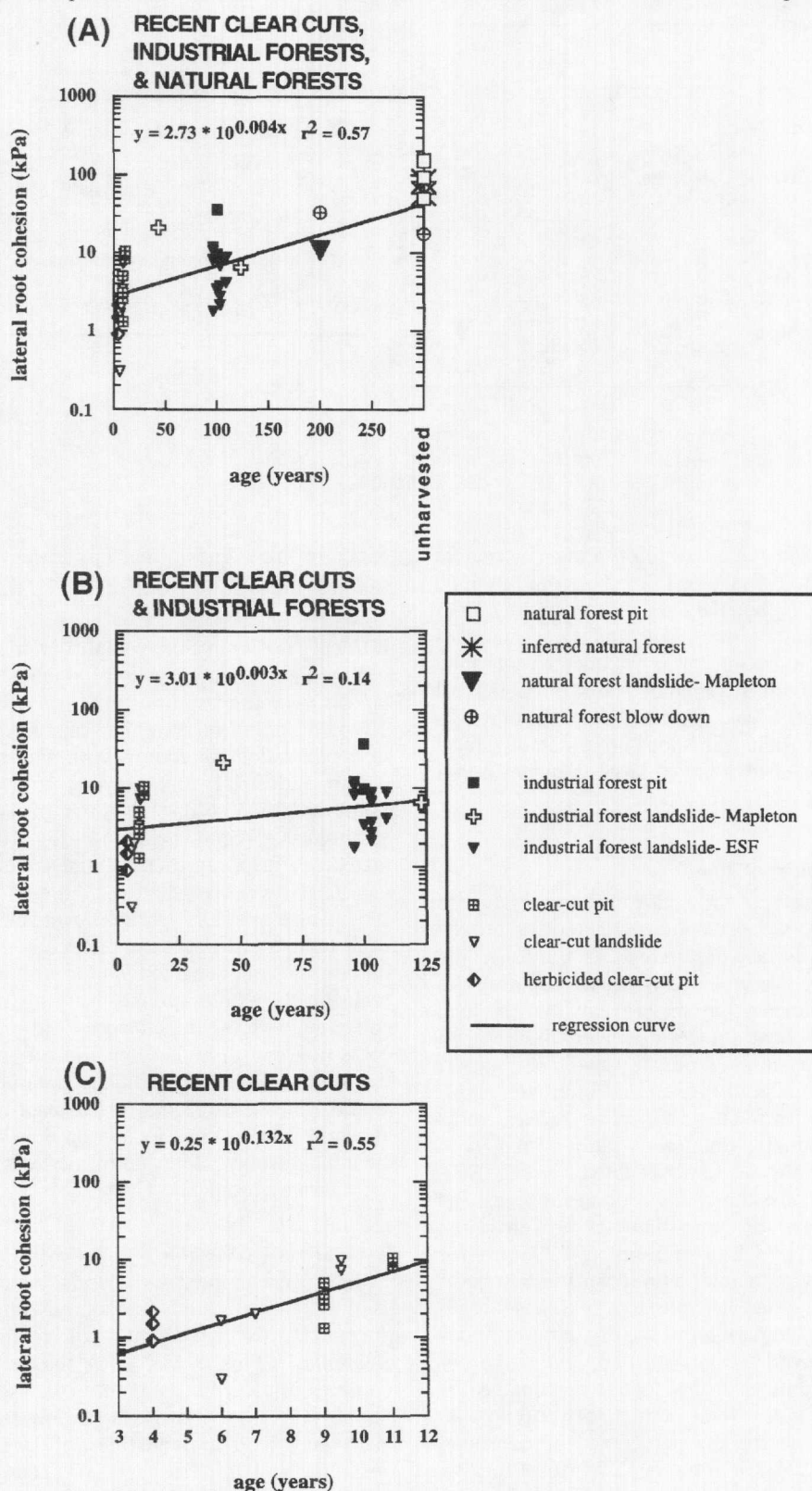
Lateral root cohesion variability in landslides

When examining roots within landslide scarps, we divided landslide perimeters into polygons of similar soil depth and a typical length of 2 m. The characteristic perimeter length of all landslides is about 25 m. The mean perimeter length within industrial forests was 16.9 m, whereas that in clearcuts was 33.6 m. The range of lateral root cohesion for each scarp polygon is shown in Fig. 10, and those values depicted in Fig. 8 represent spatially weighted means. Besides varying between vegetation communities, lateral root cohesion is also spatially variable over distances of only metres. Both industrial forests and clearcuts have a dense concentration of low root cohesion values with medians <10 kPa. Natural forests exhibit widely varying maximum lateral root cohesion, with the punctuated, local lateral cohesion maxima corresponding to higher densities of roots provided by conifers or hardwood trees. In the natural forests, for instance, lateral cohesion adjacent to vast root networks is commonly above 10 kPa and can locally approach 100 kPa. In contrast, clearcuts display values uniformly less than 25 kPa, with numerous measurements <1 kPa.

Lateral root cohesion and landslide volume

Field measurements of landslide dimensions were also used to calculate landslide source volumes. Consistent with the uniformly low values of lateral root cohesion in clearcuts in Figs. 8 and 10 is the generally greater source volumes of clear-cut landslides than landslides in industrial forests (Fig. 11). That is, larger areas of low root reinforcement may lead to landslides of larger dimensions. Curiously, a landslide situated at a cut boundary within an industrial forest has a volume more similar to those of clearcuts than to those of the remainder of the industrial forest landslides (Fig. 11). Previous research, however, indicates that source volumes are generally smaller in

Fig. 12. Lateral root cohesion as a function of time since forest-stand resetting disturbance (timber harvest, fire, or harvest and herbicide application). Regression equations and coefficients of determination (r^2) are valid for time windows expressed.
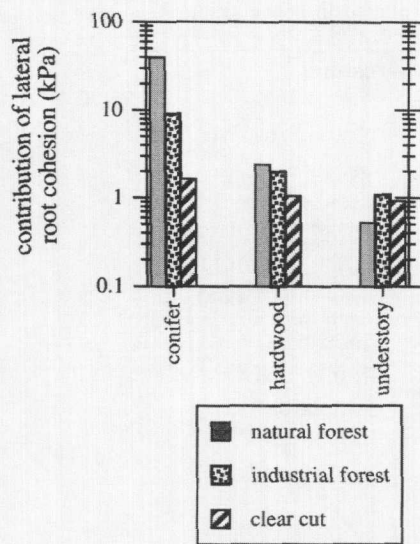

grassland and brush (where root cohesion values are consistently low) than in forests (Selby 1976; Lehre 1982; Reneau and Dietrich 1987).

Lateral root cohesion and forest stand age

Forest stand age is often used as a proxy for evaluating the influence of vegetation on slope stability. To investigate

Fig. 13. Semilogarithmic plot of mean root cohesion contribution from coniferous, hardwood, and understory vegetation for all sites.

the nature of this relationship we compared the spatially weighted lateral cohesion values depicted in Fig. 8A with time since stand disturbance. The entire time span (up to 300 years; Fig. 12A) shows a moderate relation between lateral root cohesion of all land-use types and age. In this multiple-century window the established coniferous forests express high lateral root cohesion, and the minimum values uniformly increase with an increase in age. The intermediate time span (up to 125 years; Fig. 12B) essentially shows no relation between recent clearcuts and industrial forests. The Kolmogorov–Smirnov test, discussed earlier, indicates that the industrial forest and clear-cut sites are derived from the same cumulative distribution function. Little difference exists between lateral cohesion representative of a decade after timber harvesting and that representative of a century after timber harvesting. There is, though, a solitary spike of higher cohesion values for a forest that was likely replanted with conifer seedlings 43 years prior to measuring root cohesion. Replanting conifer seedlings after harvesting, however, was not a common forestry practice a century ago. The short time span solely representative of recent clearcuts (from 0 to 12 years; Fig. 12C) again shows a modest relation between lateral root cohesion and age. The reestablishment of pioneer vegetation reveals that during the first 7 years after timber harvesting root cohesion is limited to values <3 kPa. Lateral root cohesion values >10 kPa are restricted to post-harvest, vegetation regrowth that is over 9 years in age. It appears that almost a decade is necessary for coniferous and hardwood vegetation to recover to root cohesion values >10 kPa.

Lateral root cohesion and vegetation type

Factors influencing the magnitude of lateral root cohesion expressed in Fig. 12 are the species of vegetation, density of individual plants, and diameter of roots. Figure 13 associates the mean contribution of lateral root cohesion from individual vegetation strata (i.e., conifer, hardwood, and understory) for all sites. Natural forests are dominated by coniferous
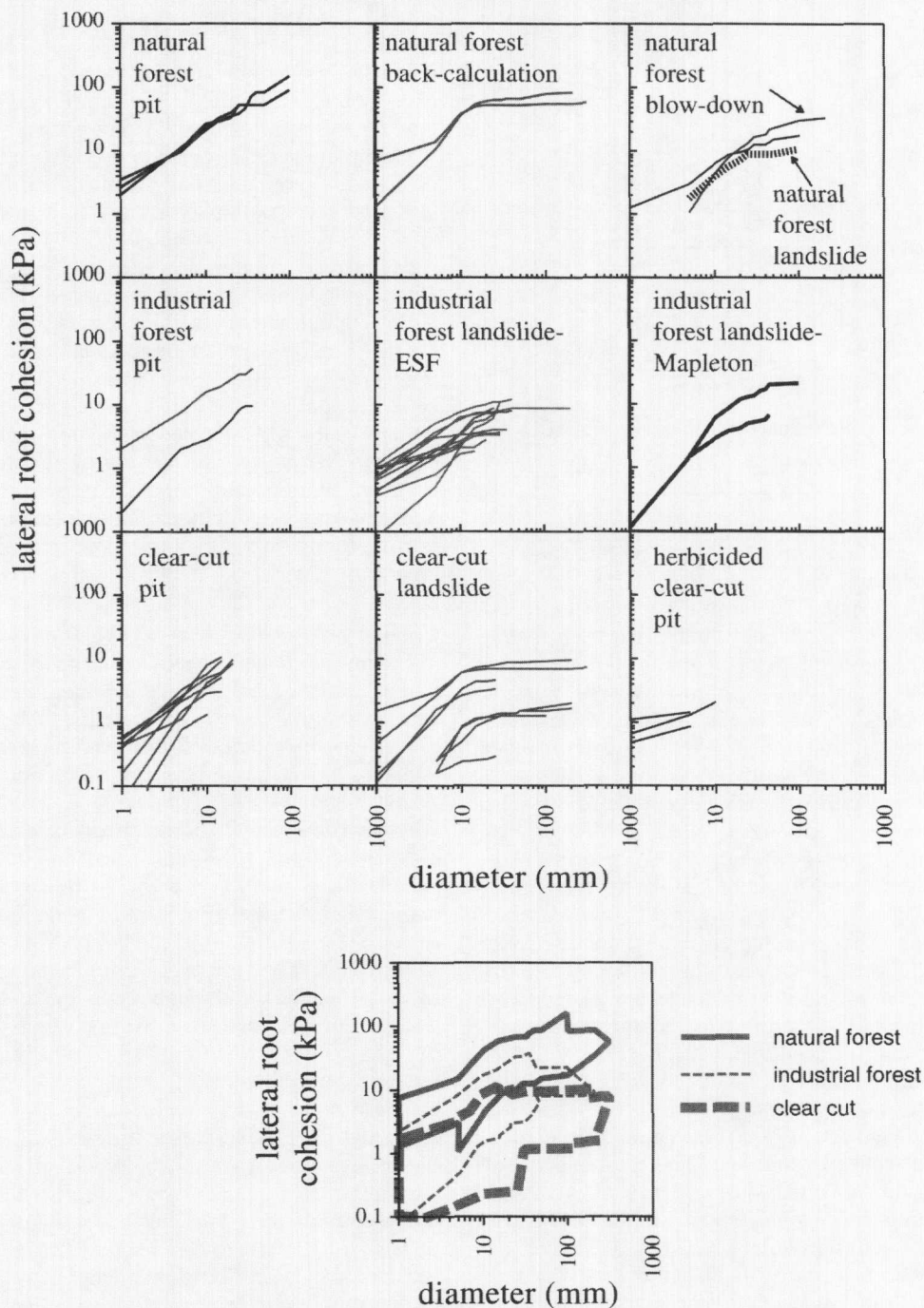
vegetation, whereas industrial forests and clearcuts express reduced contributions from coniferous vegetation. The contribution from hardwood vegetation is roughly similar for natural and industrial forests. Clearcuts receive roughly equal contribution from conifer, hardwood, and understory species. The average contribution of lateral root cohesion from the combination of hardwood and understory vegetation, though, is roughly equivalent for all land-use types: average natural forest is 2.9 kPa, average industrial forest 3.1 kPa, and average clearcut 2.0 kPa. While the component of lateral root cohesion contributed by hardwood and understory vegetation is limited to less than 12 kPa at all sites, those sites with root cohesion values over 15 kPa are dominated by coniferous vegetation (not shown in Fig. 13). Hence, industrial forestry appears to limit the contribution from coniferous vegetation, producing a shift toward a greater proportion of hardwood and understory vegetation, with the Mapleton forest characterized by a large proportion of hardwoods and the ESF having a strong understory component. Lateral root cohesion within clear-cut sites has an even smaller component arising from coniferous vegetation, with an approximately equal contribution from coniferous and understory vegetation. Thimbleberry, possessing an extensive root network, is a primary source of root cohesion in clear-cut sites.

Lateral root cohesion and root diameter

Figure 14 depicts the relationship between root diameter and lateral root cohesion at all measurement sites. Natural forests attain greater root cohesion values by having both higher densities of small-diameter roots and greater overall densities of maximum-diameter roots. For comparison, 1 mm diameter roots alone generate 1–7 kPa in natural forests, whereas roots up to 10 mm in diameter are required within clearcuts and industrial forests to attain only 1 kPa. The presence of dead roots is evident in the low plateau (~10 kPa) expressed by curves representing clear-cut landslides; large-diameter, dead roots in clearcuts provide little additional reinforcement. The summary figure at the base of Fig. 14 represents boundaries encompassing the individual curves for natural forests, industrial forests, and clearcuts. Notable overlap exists between industrial forest sites and both clear-cut and natural forests. Marginal overlap exists between clear-cut and natural forest sites.

To highlight the influence of root diameter, we normalized the contribution of lateral root cohesion for all sites within a land-use type. Figure 15 shows a distinct separation of vegetation communities with mean root diameter and the proportion of total measured cohesion. The sites represented by herbicided clear-cut pits and clear-cut pits show the smallest mean root diameters, and the natural forest pits and blowdown sites show the greatest mean root diameters. Curiously, a strong overlap exists between clear-cut landslides and industrial forest landslides in the ESF, the site of the 1960s yarding-cable thinning operation. The industrial forests in the Mapleton area exhibit diameters approaching those of natural forests. The industrial, second-growth forests in the ESF have lower root cohesion values, similar to those of recent clearcuts, because they have smaller root diameter distributions and a large proportion of understory and hardwood vegetation.

© 2001 NRC Canada

Fig. 14. Semilogarithmic plots of cumulative root cohesion and diameter distribution for different vegetation communities. The top row represents natural forests, the middle row industrial forests, and the bottom row clearcuts. Curves for individual sites are terminated at the maximum total root cohesion. Natural forests exhibit higher cohesion values for a suite of root diameters and higher maximum values. The solitary graph at the bottom of the figure represents boundaries of curves plotted in above graphs.

Root decay and regrowth

A lag time from timber harvesting to a higher frequency of landsliding is commonly associated with the decay of roots (Rice and Krammes 1970; Burroughs and Thomas 1977; Ziemer and Swanston 1977; Ziemer 1981; O'Loughlin and Ziemer 1982; Fahey et al. 1988; Hendrick and Pregitzer 1993; Fahey and Arthur 1994; Watson et al. 1999). The window of landslide hazard or response time of root decay and regrowth following disturbance, however, can differ greatly over a landscape depending on local growing conditions, lateral root growth rate, plant density, and the pioneering species of vegetation. In areas with roughly equivalent topographic and hydrologic characteristics, those sites with a long duration of suppressed root cohesion are more prone to landsliding during large-magnitude storms. Although the duration of time since harvest is critical, the species of postdisturbance vegetation plays a key role in determining the magnitude of root cohesion available. In the following cal-

Fig. 15. Proportion of total root cohesion as a function of mean root diameter for the different vegetation communities.

culations we heuristically portray two different site-specific responses to timber harvest. We use root cohesion measurements obtained just after landsliding, inferred root cohesion values representative of conditions prior to timber harvest, and the proportion of understory, hardwood, and coniferous vegetation from two sites located in close proximity to one another to illustrate how the type of vegetation influences the relative response of root cohesion to disturbance.

Total root cohesion after timber harvest is a function of (i) the declining component from the decay of roots present prior to cutting, and (ii) the increasing contribution from roots of vegetation established after cutting. For simplicity, we apply the Douglas-fir decay function in eq. [14] to all conifers and hardwoods. By assuming that the understory component available for decay at the time of cutting is zero, we therefore underestimate the total strength at the time of cutting. The contribution of root cohesion from the establishment of post-harvest root regrowth, c_{rrg} (in kPa), from understory, hardwood, and coniferous vegetation can be defined as an exponential function with the form
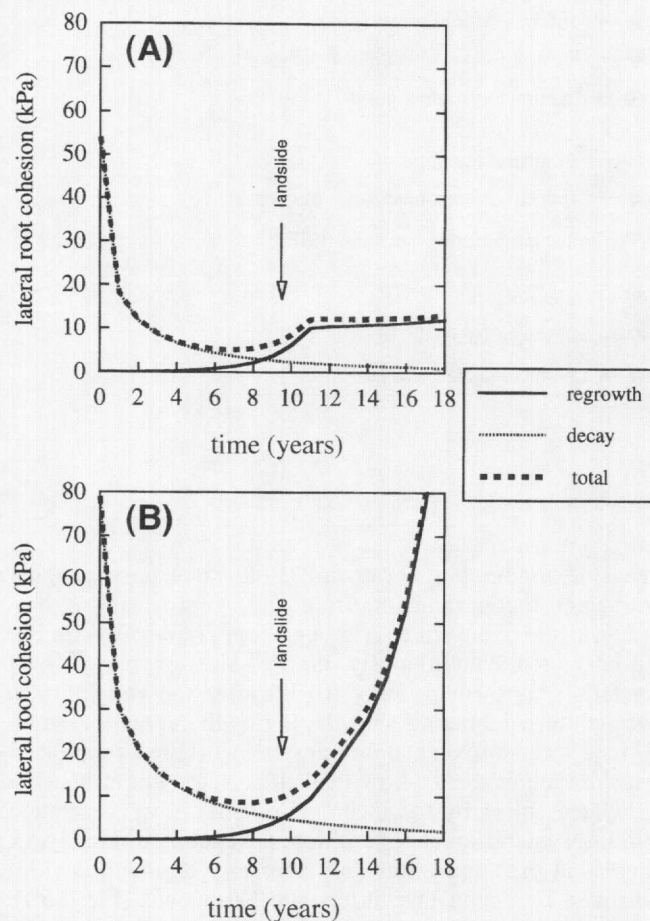
[15] $c_{rrg} = ke^{b_*t}$

where e is the base of the natural logarithm, and k and b_* are determined from the root cohesion at a given time since cutting. Sidle (1991) suggests, however, that a sigmoid relationship is more appropriate than an exponential or power function representation for vegetation regrowth after timber harvest because exponential functions generate unrealistically high root cohesion at large values of t. Based on our data set encompassing forests up to 300 years in age, a power function seems to fit clearcuts and all land-use types combined equally well (Fig. 12). From Figs. 12 and 13 we infer that the combined root cohesion of understory and hardwood vegetation attains a maximum value of about 10 kPa. Root cohesion values >10 kPa are likely a function of the presence of coniferous vegetation.

To compare variations in post-harvest vegetation, we selected two sites in the field area west of Roseburg located on the same topographic headwall. Both sites have roughly equivalent topographic controls and were clear-cut harvested at the same time. Although topographically similar and harvested synchronously, the two sites express distinct vegetation regrowth patterns. To illustrate the variability in regrowth at neighboring sites the regrowth curves (based on the first decade of vegetation reinstatement) are extrapolated past the time of the shallow landslide. Regrowth at one site is dictated solely by the incursion of understory vegetation with little establishment of coniferous vegetation (Fig. 16A), whereas at the companion site understory regrowth is complimented by abundant conifers and hardwoods (Fig. 16B). Root cohesion values at $t = 0$ are inferences of prelogging values based on diameters of observed decaying hardwood and conifer roots emanating from stumps adjacent to the slide scar. The root cohesion values at the time of landsliding are based on the measured components of decaying prelogging roots and the reestablishment of new vegetation. The timing of landsliding suggests that failure occurred shortly after the minimum value in root cohesion. Roots associated with stumps examined immediately after landsliding revealed an advanced state of decay. The inflection points expressed by the regrowth and total curves correspond to the projected time at which the understory vegetation attains the ceiling of 10 kPa inferred from Fig. 13. Root cohesion values after the time of landsliding are strictly theoretical projections based on the amount and species of vegetation present at the time cohesion was measured. The two cases reveal stark differences in the reestablishment of the same age second-growth forest. The site dominated by understory vegetation (Fig. 16A) is limited to root cohesion values <15 kPa for at least 18 years, whereas the site with abundant hardwood and conifer vegetation regenerates root cohesion to pre-cutting levels within 16 years (Fig. 16B). Thus simply inferring relative root reinforcement from a simple age designation for a given stand of vegetation may belie a more complex relationship between root reinforcement and time since disturbance.

Fig. 16. Regrowth and decay contributions of total lateral root cohesion for two sites that were clear-cut logged in 1986 and yielded landslides in 1996.

Slope stability modeling

Using site-specific field measurements of c_{rl}, A_l, z, θ, and A/b at landslide sources, we solve eq. [13] for the local hydrologic conditions, $(q/T)_c$, under varying vegetation communities (Fig. 17). All landslide sites are modeled with the following attributes: $\phi' = 40°$, c_{rl} as the site-specific value in Fig. 8A and Table 2, $c_{sl}' = c_{sb}' = c_{rb} = 0$, $\rho_w = 1000$ kg/m^3, $\rho_s = 1600$ kg/m^3, and $g = 9.81$ m/s^2. As our field observations document negligible basal root cohesion arising from roots within landslides ($c_{rb} = 0$), the term $c_b A_b$ is neglected. By adopting a high value of internal friction characteristic of low confining pressures at the ground surface, we reduce the number of sites predicted to be unstable even under dry conditions [$\tan \theta \geq \tan \phi' + (c_l A_l + c_b A_b)/(A_b \rho_s g z \cos^2 \theta)$] because all the landslides studied occurred during heavy rain. Although ρ_s varies as a function of depth below the ground surface, we use a single value of $\rho_s = 1600$ kg/m^3 to represent the saturated bulk density. As the expanded one-dimensional slope stability approximations dictate the inclusion of landslide dimensions, only landslide scarps are included. All the sites representing hand-dug pits are excluded because they do not accurately represent typical landslide dimensions; the value of A_l is set by the pit wall dimension, and A_b is undefined.
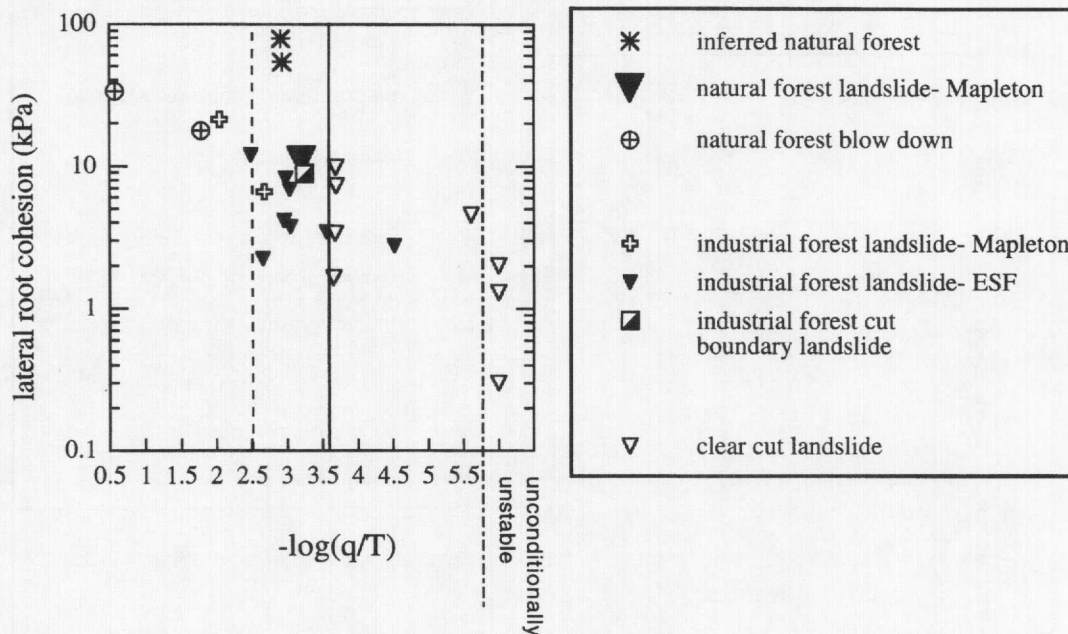
Based on site-specific attributes of hydrologic conditions, Fig. 17 displays the relative influence of both lateral root cohesion and topographic attributes on the hydrologic response. Landsliding at clear-cut sites requires higher values of $-\log(q/T)$ than industrial forest or natural forests. Although some overlap exists, a threshold value of $-\log(q/T) = 3.6$ separates landslides within clearcuts from all but one of the industrial forest landslides. Under the conditions observed, three of the clear-cut landslide sites with low root cohesion were predicted to be unconditionally unstable even under dry conditions. Assuming that the transmissivity is invariant for heuristic argument, low values of $-\log(q/T)$ correspond to high steady-state equivalent rainfall necessary to cause landsliding, and high values of $-\log(q/T)$ correspond to low critical steady-state equivalent rainfall. Clear-cut sites are both unconditionally unstable (predicted to be unstable without rainfall) and susceptible to landsliding under lower apparent rainfall intensities. The occurrence of landslides from clearcuts during frequent, low-rainfall storms is consistent with field observations by Montgomery et al. (2000). Alternatively, landslides representative of natural forests possess lower values of $-\log(q/T)$ and hence require higher apparent rainfall intensities to initiate landsliding. The lower $-\log(q/T)$ bound to the industrial forest landslides occurs at a value of about 2.5.

Viewed slightly differently, the proportion of the saturated regolith required to cause instability in different vegetation communities can be examined with respect to local root cohesion. Equation [10] expresses a positive relationship between M_c and c_l which is modified by the site-specific values of A_l, A_b, θ, and z. Assuming slope-parallel groundwater flow, Fig. 18 shows that almost all the clear-cut sites require less than half of the regolith to be saturated to trigger landsliding. Three of the clear-cut landslide sites with low root cohesion were predicted to be unconditionally unstable even under dry conditions. In contrast, values of M_c range from 0.004 to 2.8 for industrial forests and from 1.25 to 16.4 for natural forests. Thus all clear-cut and most industrial forest landslides could initiate under low values of M_c, whereas sites in natural forests require high values of M_c to trigger landsliding. Hence areas with high cohesion values may require locally concentrated exfiltrating flow from the underlying bedrock into the colluvium or nonslope-parallel flow within the colluvium to trigger landsliding. Considering the limitations of the model assumptions, the values of M_c are intended only to elucidate the relative hydrologic response necessary to induce landsliding, and not to represent actual values.

Discussion

In the Oregon Coast Range, lateral root reinforcement of soil greatly exceeds basal reinforcement. Calculation of slope stability using simple infinite slope approximations, though, neglects substantial reinforcement from roots that are oriented slope-parallel. Unfortunately, there are few published values of lateral root cohesion because the majority of published reports using in situ direct shear tests and back-calculation techniques assume all roots anchor the basal surface of a landslide into the underlying bedrock. See Table 4 for comparison of the lateral root cohesion values reported

Fig. 17. Semilogarithmic plot of lateral root cohesion and back-calculated hydrologic properties, $-\log(q/T)$. Vertical lines from left to right represent $-\log(q/T) = 2.5$, $-\log(q/T) = 3.6$, and the limit of unconditionally unstable conditions.

here (Table 2; Fig. 8) with both basal and lateral root cohesion values reported previously for similar vegetation assemblages.

Our field data demonstrate that lateral root cohesion within a given vegetation community and root cohesion variability between different land-use types exceed the variability within a given land-use type. For instance, median root cohesion is lower for clearcuts and herbicided clearcuts than for natural forests (Table 2; Fig. 8). In addition, the spatial variability of maximum root cohesion values along landslide perimeters within clearcuts is a great deal less than that within natural and industrial forests (Fig. 10). Thus, if shallow landslides occur at gaps in the root network, clearcuts and industrial forests have a greater landslide susceptibility because they possess wider gaps and lower overall root cohesion. Furthermore, if landslides in clearcuts tend to have larger initial source volumes (Fig. 11), they may trigger long run-out debris flows. This association highlights the importance of well-established understory and hardwood vegetation in industrial forests to provide a spatially continuous root mat. Understory vegetation in recent clearcuts (<11 years old) attain maximum root cohesion values of about 10 kPa (Figs. 8, 12; Table 2), a value that may greatly increase stability. Field observations of reduced root cohesion following herbicide application, in conjunction with modeling results by Sidle (1992) indicating that the suppression of understory vegetation drastically reduces slope stability, demonstrate a high likelihood of lower values of root cohesion persisting for longer periods of time following herbicide application after logging.
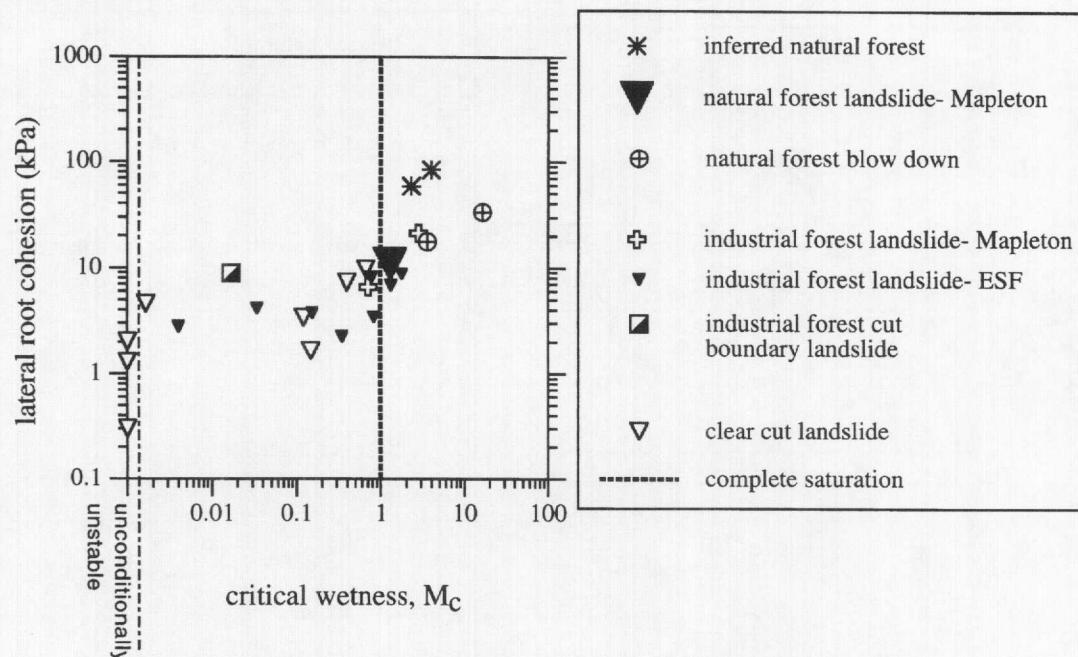
Certain industrial forests exhibit root area ratios (Fig. 7), lateral root cohesion (Table 2; Fig. 8), species associations (Fig. 13), and root diameter distributions (Figs. 14, 15) which more closely resemble clearcuts than natural forests. The disturbance legacy within industrial forests arises from previous clearcuts and selective timber harvesting, fires set

intentionally to flush game and clear vegetation, and the introduction of non-native vegetation, insects, and diseases. The overlap in root cohesion values between industrial forests and clearcuts (Fig. 8) may indicate that landslides initiate from industrial forests at a higher rate because they possess a vegetative cover characterized by relatively low root cohesion or large gaps at potential landslide source locations.

Role of legacy

Reduced values of lateral root cohesion may persist for at least a century. Root cohesion of 10-year-old forests is possibly similar to values from 100-year-old forests (Fig. 12) because forestry practices a century prior did not replant conifer seedlings following timber harvest. Therefore much of the root cohesion in 100-year-old forests originates from hardwood and understory vegetation. Although roots of hardwood and understory vegetation have root strengths similar to that of coniferous vegetation (Fig. 5), they typically have smaller maximum diameters (Figs. 14, 15). Even though 100-year-old forests could be considered as being established, there appears to be a significant difference between root cohesion values representative of the background condition in a natural forest and the anthropogenically influenced value of root cohesion in industrial forests. Some areas in the ESF that were cut around the year 1900, for example, presently maintain a monoculture of red alder of moderate diameters. Based on the species of stumps, this replaces a mixed conifer forest of Douglas-fir and red cedar with large diameters (Table 3). More recently, damage from yarding-cables and the removal of trees during thinning operations persists for at least 30 years. A study by Zavitkovski and Stevens (1972) in the Oregon Coast Range documents that the dry weight of red alder roots decreases for trees >60 years old. Hence, landslide susceptibility may increase in

© 2001 NRC Canada

Fig. 18. Logarithm–logarithm plot showing a rough positive correlation between lateral root cohesion and critical wetness, M_c, necessary to initiate landsliding. The bold, broken line represents the complete saturation of colluvium.

areas such as the ESF dominated by a large proportion of >60-year-old red alder trees with decreased root area ratios.

Land management implications

To assess shallow landslide susceptibility in forested hillslopes with different land-use histories, the spatial variability of root cohesion in addition to vegetation age should be appraised. The relative productivity of a forest, and hence the underlying root cohesion governing landslide susceptibility, is not simply a function of time since harvesting. Although Fig. 12 reveals a general relationship between root cohesion and time since stand-resetting disturbance, labeling forest stands simply by the age of the oldest living tree obscures the local history of the land while contributing only partial insight into the extent of root reinforcement regulating local landslide susceptibility. In the context of slope stability, stand age classifications should be augmented with insight into the magnitude of local variability within the stand condition. That is, uniform characterizations of root cohesion representative of generalized age of vegetation may be less informative than determining the local, site-specific species assemblages and density.

The window of landslide hazard is a function of the magnitude of the hydrologic response and the decay time to a root cohesion low enough to allow for landsliding and the time spent below the critical value (Ziemer and Swanston 1977; Ziemer 1981). In areas of equivalent material strength and topographic and hydrologic settings, the temporal window of high landslide hazard is shorter where vegetation becomes quickly established. The planting of conifer seedlings immediately post-cutting should act to narrow the window. As a gauge of the duration of this window, previous research reports it may take 15 to more than 25 years for a regenerating clear-cut lodgepole pine forest in California to restore 50% of its original root strength (Ziemer 1981). In New Zea-

land, Watson et al. (1999) demonstrate how plant species exhibiting specific rooting habits can be used to control erosion. Watson et al. discuss how information on live root strength, decay rates, and root growth habits of radiata pine (*Pinus radiata*) and kanuka (*Kunzea ericoides*) can be used to narrow the window of landslide hazard. Kanuka root threads express the unique quality that they temporarily increase in tensile strength after timber harvest and express slower rates of subsequent root decay. The kanuka roots provide cohesion during the critical period when new roots are becoming established. As revealed in Fig. 16, the window of landslide hazard marked by low root cohesion values can be tied strongly to site-specific conditions and species distributions. The window of landslide hazard may be greater for industrial forests where initial root cohesion values are lower and the subsequent exponential decline of root cohesion to critical values occurs over a shorter time period. In addition, the interval between present commercial harvest cycles may be shorter than the time necessary for root cohesion to recover to background levels characteristic of natural forests.

In the context of slope stability modeling, the implications of high spatial and temporal variability in root cohesion values are tremendous. Typical regional landslide hazard analyses either impose a given, uniform value of cohesion across the landscape or bracket high and low values of cohesion. Bracketing cohesion values furnishes the best- and worst-case scenarios but cannot reliably locate specific regions producing landslides in a given storm. Root cohesion data of the type presented here can help to identify specific landslide hazards, but field measurements are time consuming and thus aid little in regional-scale predictions. When comparing predictions of regional slope stability to mapped landslides resulting from a given storm, site-specific variations of not only root reinforcement but also variations in soil depth, material properties, and hydrologic routing gov-

ern why certain areas of high predicted hazard produce landslides while other areas of high predicted hazard do not.

Conclusions

Detailed measurements at many landslides that occurred during the 1996 storms in the Oregon Coast Range indicate that measurements of root reinforcement must be compiled at the landslide scale because the vegetation and root cohesion vary at that scale. This variation in root cohesion between different vegetation communities is significant but quantifiable. We measured root area ratio, thread diameter, species of vegetation, and proportion of live roots as the salient vegetation characteristics controlling root cohesion in the Oregon Coast Range. Although root area ratios of both live and decaying roots are similar for all the vegetation communities, root area ratios representative of live roots are greatly reduced in clearcuts and industrial forests. We find that median lateral root cohesion of unharvested old-growth forests (25.6–94.3 kPa) exceeds that of industrial forests (6.8–23.2 kPa) up to 123 years old. In some industrial forests, the dominance of hardwood and understory vegetation arises from the legacy of prior forest practices, reducing root cohesion at potential landslide-initiation sites. This suppressed root cohesion within industrial forests likely reflects the local history or disturbance legacy arising from fire, commercial thinning, or partial conversion of conifer to hardwood forest. In some localities, root cohesion recovery may be arrested by dense understory and hardwood vegetation that creates zones of reduced root strength which may last for at least a century. Median lateral root cohesion in clearcuts <11 years old has even lower values of 1.5–6.7 kPa, consistent with calculations that indicate the conversion of old-growth, unharvested forests to industrial forests should trigger significant increases in the rates of landsliding. Even though <11-year-old clearcuts have root cohesion values ranging up to 10 kPa, simulations that couple the idealized hydrologic routing and the expanded one-dimensional slope stability models indicate that clearcuts are more susceptible to landsliding than either industrial or natural forests. Data on some herbicided clear-cut sites indicate that the practice of herbiciding further decreases root cohesion, acting to extend the window of landslide hazard.

The conversion of old-growth, unharvested forests to industrial forests may trigger significant increases in the rates of landsliding, although significant spatial variability should be expected because landslide susceptibility is extremely site dependent. We conclude that a refined classification of vegetation is necessary to augment stand age designations to establish the intricate association between landsliding and vegetation. In addition to the variability in hydrologic response, we speculate that some of the apparent stochastic nature of landslide occurrence during individual storms may reflect quantifiable variations in root strength at the scale of individual landslide sites. Future research surrounding these issues could utilize data on the density of timber per given area or remote-sensing information, such as mapping canopy structure using laser altimetry, to characterize the amount of root cohesion and its spatial variability in a geographic information system. Such an approach could be used to better assess risks posed by timber harvest plans in landslide-prone landscapes.

References

Abe, K., and Iwamoto, M. 1986. An evaluation of tree-root effect on slope stability by tree-root strength. Journal of the Japanese Forestry Society (Nippon Rin Gakkaishi), **69**: 505–510.

Amaranthus, M.P., Rice, R.M., Barr, N.R., and Ziemer, R.R. 1985. Logging and forest roads related to increased debris slides in southwestern Oregon. Journal of Forestry, **83**: 229–233.

Anderson, C.J., Coutts, M.P., Ritchie, R.M., and Campbell, D.J. 1989. Root extraction force measurements for Sitka Spruce. Forestry, **62**: 127–137.

Bannan, M.W. 1940. The root systems of northern Ontario conifers growing in sand. American Journal of Botany, **27**: 108–114.

Bishop, D.M., and Stevens, M.E. 1964. Landslides on logged areas in southeast Alaska. U.S. Forest Service, Northern Forest Experiment Station, Research Paper NOR-1.

Böhm, W. 1979. Methods of studying root systems. Ecological Series. Springer-Verlag, Berlin, Germany.

Brown, G.W., and Krygier, J.T. 1971. Clear-cut logging and sediment production in the Oregon Coast Range. Water Resources Research, **7**: 1189–1199.

Buchanan, P., and Savigny, K.W. 1990. Factors controlling debris avalanche initiation. Canadian Geotechnical Journal, **27**: 659–675.

Burroughs, E.R.J. 1985. Landslide hazard rating for the Oregon Coast Range. *In* Watershed management in the eighties. *Edited by* E.B. Jones and T.J. Ward. American Society of Civil Engineers, New York, pp. 132–139.

Burroughs, E.R.J., and Thomas, B.R. 1977. Declining root strength in Douglas-fir after felling as a factor in slope stability. U.S. Forest Service, Research Paper INT-190.

Carrara, A., Cardinali, M., Detti, R., Guzzetti, F., Pasqui, V., and Reichenback, P. 1991. GIS techniques and statistical models in evaluating landslide hazard. Earth Surface Processes and Landforms, **16**: 427–445.

Commandeur, P.R., and Pyles, M.R. 1991. Modulus of elasticity and tensile strength of Douglas-fir roots. Canadian Journal of Forestry Research, **21**: 48–52.

Coppin, N.J., and Richards, I.G. (*Editors*). 1990. Use of vegetation in civil engineering. Construction Industry Research and Information Association, Butterworths, London.

Corliss, J.F. 1973. Soils survey of Alsea area, Oregon. U.S. Soil Conservation Service Soil Survey, U.S. Federal Government.

Coutts, M.P. 1983. Root architecture and tree stability. Plant and Soil, **71**: 171–188.

Cruden, D.M., and Varnes, D.J. 1996. Landslide types and processes. *In* Landslides investigation and mitigation. *Edited by* A.K. Turner and R.L. Schuster. Transportation Research Board, National Research Council, Special Report 247, pp. 36–75.

Deans, J.D., and Ford, E.D. 1983. Modelling root structure and stability. Plant and Soil, **71**: 189–195.

DeGraff, J.V. 1979. Initiation of shallow mass movement by vegetative-type conversion. Geology, **7**: 426–429.

Dietrich, W.E., and Dunne, T. 1978. Sediment budget for a small catchment in mountainous terrain. Zeitschrift für Geomorphologie, Supplementband, **29**: 191–206.

Dietrich, W.E., Wilson, C.J., Montgomery, D.R., McKean, J., and Bauer, R. 1992. Erosion thresholds and land surface morphology. Geology. **20**: 675–689.

Dietrich, W.E., Wilson, C.J., Montgomery, D.R., and McKean, J. 1993. Analysis of erosion thresholds, channel networks, and landscape morphology using a digital terrain model. Journal of Geology, **101**: 259–278.

Dietrich, W.E., Reiss, R., Hus, M.-L., and Montgomery, D.R. 1995. A process-based model for colluvial soil depth and shallow landsliding using digital elevation data. Hydrological Processes, **9**: 383–400.

Dott, R.H.J. 1966. Eocene deltaic sedimentation at Coos Bay, Oregon. Journal of Geology, **74**: 373–420.

Eis, S. 1974. Root system morphology of Western Hemlock, Western Red Cedar, and Douglas-fir. Canadian Journal of Forestry Research, **4**: 28–38.

Eis, S. 1987. Root systems of older immature hemlock, cedar, and Douglas-fir. Canadian Journal of Forestry, **17**: 1348–1354.

Ellen, S.D., Mark, R.K., Cannon, S.H., and Knifong, D.L. 1993. Map of debris-flow hazard in the Honolulu District of Oahu, Hawaii. U.S. Geological Survey, Open-file Report 93-213.

Endo, T., and Tsuruta, T. 1969. Effects of tree's roots upon the shearing strengths of soils. *In* 18th Annual Report of the Hokkaido Branch, Government Forest Experimental Station, Tokyo, pp. 167–179.

Ennos, A.R. 1990. The anchorage of leek seedlings: the effect of root length and soil strength. Annals of Botany, **65**: 409–416.

Fahey, T.J., and Arthur, M.A. 1994. Further studies of root decomposition following harvest of a northern hardwoods forest. Forest Science, **40**: 618–629.

Fahey, T.J., Hughes, J.W., Pu, M., and Arthur, M.A. 1988. Root decomposition and nutrient flux following whole-tree harvest of northern hardwood forest. Forest Science, **34**: 744–768.

Franklin, J.F., and Dyrness, C.T. 1969. Vegetation of Oregon and Washington. U.S. Forest Service, Research Paper PNW-80.

Gray, D.H., and Leiser, A.T. 1982. Biotechnical slope protection and erosion control. Van Nostrand Reinhold Co., New York.

Gray, D.H., and Megahan, W.F. 1981. Forest vegetation removal and slope stability in the Idaho Batholith. U.S. Forest Service, Research Paper INT-271.

Gray, D.H., and Ohashi, H. 1983. Mechanics of fiber reinforcement in sand. Journal of Geotechnical Engineering, ASCE, **109**: 335–353.

Gresswell, S., Heller, D., and Swanston, D.N. 1979. Mass movement response to forest management in the central Oregon Coast Ranges. U.S. Forest Service, Resource Bulletin PNW-84.

Haagen, J.T. 1989. Soil survey of Coos Country, Oregon. U.S. Soil Conservation Service Soil Survey, U.S. Federal Government.

Hathaway, R.L., and Penny, D. 1975. Root strength in some

Populus and *Salix* clones. New Zealand Journal of Botany, **13**: 333–344.

Hendrick, R.L., and Pregitzer, K.S. 1993. Patterns of fine root mortality in two sugar maple forests. Nature (London), **361**: 59–61.

Ifju, G., and Kennedy, R.W. 1962. Some variables affecting microtensile strength of Douglas-fir. Forest Products Journal, **12**: 213–217.

Jewell, R.A., and Wroth, C.P. 1987. Direct shear tests on reinforced sand. Géotechnique, **37**: 53–68.

Kassiff, G., and Kopelovitz, A. 1968. Strength properties of soil–root systems. Report number CV-256, Israel Institute of Technology, Haifa, Israel.

Ketcheson, G.L., and Froehlich, H.A. 1978. Hydrology factors and environmental impacts of mass soil movements in the Oregon Coast Range. Water Resources Research Institute, Oregon State University, Corvallis.

Kochenderfer, J.N. 1973. Root distribution under some forest types native to West Virginia. Ecology, **54**: 445–448.

Krogstad, F. 1995. A physiology and ecology based model of lateral root reinforcement of unstable hillslopes. M.Sc. thesis, University of Washington, Seattle, Wash.

Kuruppuarachchi, T., and Wyrwoll, K.-H. 1992. The role of vegetation clearing in the mass failure of hillslopes: Moresby Ranges, Western Australia. Catena, **19**: 193–208.

Lehre, A.K. 1982. Sediment mobilization and production from a small mountain catchment: Lone Tree Creek, Marin Country, California. Ph.D. thesis, University of California, Berkeley, Calif.

Lovell, J.P.B. 1969. Tyee formation: undeformed turbidites and their lateral equivalents: mineralogy and paleogeology. Geological Society of America Bulletin, **80**: 9–22.

McMinn, R.G. 1963. Characteristics of Douglas-fir root systems. Canadian Journal of Botany, **41**: 105-122.

Montgomery, D.R., and Dietrich, W.E. 1994. A physically based model for the topographic control on shallow landsliding. Water Resources Research, **30**: 1153–1171.

Montgomery, D.R., Dietrich, W.E., Torres, R., Anderson, S.P., Heffner, J.T., and Loague, K. 1997. Hydrologic response of a steep, unchanneled valley to natural and applied rainfall. Water Resources Research, **33**: 91–109.

Montgomery, D.R., Sullivan, K., and Greenberg, H.M. 1998. Regional test of a model for shallow landsliding. Hydrological Processes, **12**: 943–955.

Montgomery, D.R., Schmidt, K.M., Greenberg, H.M., and Dietrich, W.E. 2000. Forest clearing and regional landsliding. Geology, **28**: 311–314.

O'Loughlin, C., and Ziemer, R.R. 1982. The importance of root strength and deterioration rates upon edaphic stability in steepland forests. *In* Carbon uptake and allocation in subalpine ecosystems as a key to management. *Edited by* R.H. Waring. Oregon State University, Corvallis, Oreg., pp. 70–78.

O'Loughlin, C.L. 1974. The effect of timber removal on the stability of forest soils. Journal of Hydrology (N.Z.), **13**: 121–134.

O'Loughlin, E.M. 1986. Prediction on surface saturation zones in natural catchments by topographic analysis. Water Resources Research, **22**: 794–804.

Phillips, C.J., and Watson, A.J. 1994. Structural tree root research in New Zealand: a review. Science Series No. 7, Landcare Research, Lincoln, Canterbury, New Zealand.

Pierson, T.C. 1977. Factors controlling debris-flow initiation on forested hillslopes in the Oregon Coast Ranges. Ph.D. thesis, University of Washington, Seattle, Wash.

Press, W.H., Teukolsky, S.A., Vetterling, W.T., and Flannery, B.P. 1992. Numerical recipes in C, the art of scientific computing. Cambridge University Press, Cambridge, Mass.

Reneau, S.L., and Dietrich, W.E. 1987. Size and location of colluvial landslides in a steep forested landscape. *In* Erosion and sedimentation in the Pacific Rim. *Edited by* R.L. Beschta, T. Blinn, G.E. Grant, G.G. Ice, and F.J. Swanson. International Association of Hydrological Sciences, Publication 165, pp. 39–48.

Rice, R.M., and Krammes, J.S. 1970. Mass wasting processes in watershed management. *In* Proceedings of the Symposium on Interdisciplinary Aspects of Watershed Management. American Society of Civil Engineers, New York, pp. 231–260.

Riestenberg, M.M. 1987. Anchoring of thin colluvium on hillslopes by roots of sugar maple and white ash. Ph.D. thesis, University of Cincinnati, Cincinnati, Ohio.

Riestenberg, M.M. 1994. Anchoring of thin colluvium by roots of sugar maple and white ash on hillslopes in Cincinnati. U.S. Geological Survey, Bulletin 2059-E.

Riestenberg, M.M., and Sovonick-Dunford, S. 1983. The role of woody vegetation in stabilizing slopes in the Cincinnati area, Ohio. Geological Society of America Bulletin, **15**: 3–45.

Rigg, G.G., and Harrar, E.S. 1931. The root systems of trees growing in sphagnum. American Journal of Botany, **18**(6): 391–397.

Robison, E.G., Mills, K., Paul, J., Dent, L., and Skaugset, A. 1999. Oregon Department of Forestry storm impacts and landslides of 1996: final report. Oregon Department of Forestry, Forest Practices Technical Report 4.

Ross, C.R. 1932. Root development of western conifers. M.Sc. thesis, University of Washington, Seattle, Wash.

Schietchtl, H.M. 1980. Bioengineering for land reclamation and conservation. University of Alberta Press, Edmonton, Alta.

Schmidt, K.M. 1999. Root strength, colluvial soil depth, and colluvial transport on landslide-prone hillslopes. Ph.D. thesis, University of Washington, Seattle, Wash.

Schroeder, W.L., and Alto, J.V. 1983. Soil properties for slope stability analysis; Oregon and Washington Coastal Mountains. Forest Science, **29**: 823–833.

Selby, M.J. 1976. Slope erosion due to extreme rainfall: a case study from New Zealand. Geografiska annaler, Series A, **58**: 131–138.

Shewbridge, S.E., and Sitar, N. 1989. Deformation characteristics of reinforced sand in direct shear. Journal of Geotechnical Engineering, ASCE, **115**: 1134–1147.

Shewbridge, S.E., and Sitar, N. 1990. Deformation-based model for reinforced sand. Journal of Geotechnical Engineering, ASCE, **116**: 1153–1170.

Sidle, R.C. 1991. A conceptual model of changes in root cohesion in response to vegetation management. Journal of Environmental Quality, **20**: 43–52.

Sidle, R.C. 1992. A theoretical model of the effects of timber harvesting on slope stability. Water Resources Research, **28**: 1897–1910.

Sidle, R.C., and Swanston, D.N. 1982. Analysis of a small debris slide in coastal Alaska. Canadian Geotechnical Journal, **19**: 167–174.

Sidle, R.C., Pearce, A.J., and O'Loughlin, C.L. 1985. Hillslope stability and land use. Water Resources Monograph Series 11, American Geophysical Union, Washington, D.C.

Smith, J.H. 1964. Root spread can be estimated from crown width of Douglas fir, Lodgepole pine, and other British Columbia tree species. Forestry Chronicle, **40**: 456–473.

Stokes, A., and Mattheck, C. 1996. Variation of wood strength in tree roots. Journal of Experimental Botany, **47**: 693–699.

Stolzy, L.H., and Barley, K.P. 1968. Mechanical resistance encountered by roots entering compact soils. Soil Science, **105**: 297–301.

Stone, E.L., and Kalisz, P.J. 1991. On the maximum extent of tree roots. Forest Ecology and Management, **46**: 59–102.

Stout, B.B. 1956. Studies of the root systems of deciduous trees. Black Rock Forest Bulletin 15, Harvard University, Cambridge, Mass.

Swanson, F.J., Swanson, M.M., and Woods, C. 1977. Inventory of mass erosion in the Mapleton Ranger District, Suislaw National Forest. Forest Science Laboratory, Corvallis, Oreg.

Swanson, F.J., Swanson, M.M., and Woods, C. 1981. Analysis of debris-avalanche erosion in steep forest lands: an example from Mapleton, Oregon, USA. *In* Erosion and sediment transport in Pacific Rim steeplands. *Edited by* T.R.H. Davies and A.J. Pearce. International Association of Hydrological Sciences, Publication 132, pp. 67–75.

Swanston, D.N. 1970. Mechanics of debris avalanching in shallow till soils of southeast Alaska. U.S. Forest Service, Research Paper PNW-103.

Swanston, D.N. 1988. Timber harvest and progressive deformation of slopes in southwestern Oregon. Bulletin of the Association of Engineering Geologists, **25**: 371–381.

Swanston, D.N., and Swanson, E.J. 1976. Timber harvesting, mass erosion, and steepland forest geomorphology in the Pacific Northwest. *In* Geomorphology and engineering. *Edited by* D.R. Coates. Dowden, Hutchinson and Ross, Inc., Stroudsburg, Pa., pp. 199–221.

Taylor, G. 1997. Causes of the flood and a comparison to other climate events. *In* The Pacific Northwest floods of February 6-11, 1996, Proceedings of the Pacific Northwest Water Issues Conference. *Edited by* A. Laenen. American Institute of Hydrology, Portland, Oreg., pp. 3–7.

Terwilliger, V.J., and Waldron, L.J. 1991. Effects of root reinforcement on soil-slip patterns in the Transverse Ranges of southern California. Geological Society of America Bulletin, **103**: 775–785.

Terzaghi, K. 1950. Mechanism of landslides. *In* Application of geology to engineering practice. *Edited by* S. Paige. Geological Society of America, New York, pp. 83–123.

Waldron, L.J. 1977. The shear resistance of root-permeated homogenous and stratified soil. Soil Science Society of America Journal, **41**: 843–849.

Waldron, L.J., and Dakessian, S. 1981. Soil reinforcement by roots: calculation of increased soil shear resistance from root properties. Soil Science, **132**: 427–435.

Waldron, L.J., and Dakessian, S. 1982. Effect of grass, legume, and tree roots on soil shearing resistance. Soil Science Society of America Journal, **46**: 894–899.

Waldron, L.J., Dakessian, S., and Nemson, J.A. 1983. Shear resistance enhancement of 1.22-meter diameter soil cross sections by pine and alfalfa roots. Soil Science Society of America Journal, **47**: 9–14.

Walker, G.W., and MacLeod, N.S. 1991. Geologic map of Oregon. U.S. Geological Survey, Special Geologic Map, scale 1 : 500 000.

Watson, A., and O'Loughlin, C. 1990. Structural root morphology and biomass of the three age-classes of *Pinus Radiata*. New Zealand Journal of Forestry Science, **20**: 97–110.

Watson, A., Phillips, C., and Marden, M. 1999. Root strength, growth, and rates of decay: root reinforcement changes of two tree species and their contribution to slope stability. Plant and Soil, **217**: 39–47.

Wu, T.H. 1976. Investigation of landslides on Prince of Wales Island, Alaska. Geotechnical Engineering Report 5, Department of Civil Engineering, Ohio State University, Columbia, Ohio.

Wu, T.H. 1984a. Effect of vegetation on slope stability. *In* Soil reinforcement and moisture effects on slope stability. Transportation Research Board, Washington, D.C., pp. 37–46.

Wu, T.H. 1984b. Soil movements on permafrost slopes near Fairbanks, Alaska. Canadian Geotechnical Journal, **21**: 699–709.

Wu, T.H. 1995. Slope stabilization. *In* Slope stabilization and erosion control: a bioengineering approach. *Edited by* R.P.C. Morgan and R.J. Rickson. E. & F.N. Spon, London, pp. 221–264.

Wu, W., and Sidle, R.C. 1995. A distributed slope stability model for steep forested basins. Water Resources Research, **31**: 2097–2110.

Wu, T.H., McKinnell, W.P., III, and Swanston, D.N. 1979. Strength of tree roots and landslides on Prince of Wales Island, Alaska. Canadian Geotechnical Journal, **16**: 19–33.

Wu, T.H., Beal, P.E., and Lan, C. 1988*a*. In-situ shear rest of soil–root systems. Journal of Geotechnical Engineering, ASCE, **114**: 1376–1394.

Wu, T.H., McOmber, R.M., Erb, R.T., and Beal, P.E. 1988*b*. Study of soil–root interaction. Journal of Geotechnical Engineering, ASCE, **114**: 1351–1375.

Yee, C.S., and Harr, D.R. 1977. Influence of soil aggregation on slope stability in the Oregon Coast Range. Environmental Geology, **1**: 367–377.

Zavitkovski, J., and Stevens, R.D. 1972. Primary productivity of red alder ecosystems. Ecology, **53**: 235–242.

Ziemer, R.R. 1981. Roots and the stability of forested slopes. *In* Erosion and sediment transport in Pacific Rim steeplands. *Edited by* T.R.H. Davies and A.J. Pearce. International Association of Hydrological Sciences, Publication 132, pp. 343–361.

Ziemer, R.R., and Swanston, D.N. 1977. Root strength changes after logging in southeast Alaska. U.S. Forest Service, Research Note PNW-306.